Langmuir and electron solitary wave at high-latitude magnetopause

B. Popielawska (1), Y. Khotyaintsev (2), J. Pickett (3), Ch. Farrugia (4), B. Kellett (5), G. Gustafsson (2), and K. Stasiewicz (2)

1) Space Research Center, Warsaw, Poland
2) Swedish Institute of Space Physics, Uppsala Division, Uppsala, Sweden
3) University of New Hampshire, Durham, NH, USA
4) University of Iowa, Iowa City, IA, USA
5) Rutherford Appleton Laboratory, Chilton, Didcot , UK

e-mail:bpop@cbk.waw.pl

Praha, IB2003 Conference, September 11, 2003

Subtitle: From milliseconds to minutes or

cross-scale coupling

in the solar-wind magnetosphere interaction

Polar, 11 April 1997, magnetopause poleward of the cusp under strong northward IMF

- **macroscale - minutes**: sunward convection at high-latitudes (***Le, G., et al., 2001***)

- **mesoscale - seconds**: D-shaped ion beams in the boundary layer (***Russell et al., 2000, Fuselier et al., 2000***), magnetic "bubbles" a the magnetopause, kinetic Alfvén waves, tearing instability of MP current layer (***Stasiewicz et al., 2002***), hydrid simulations;

→ B_n different from zero, S-shaped hodograms - thin current layer, open magnetopause

→ • **microscale - milliseconds**: LH waves, whistlers, electron solitary waves, and finally, Langmuir waves

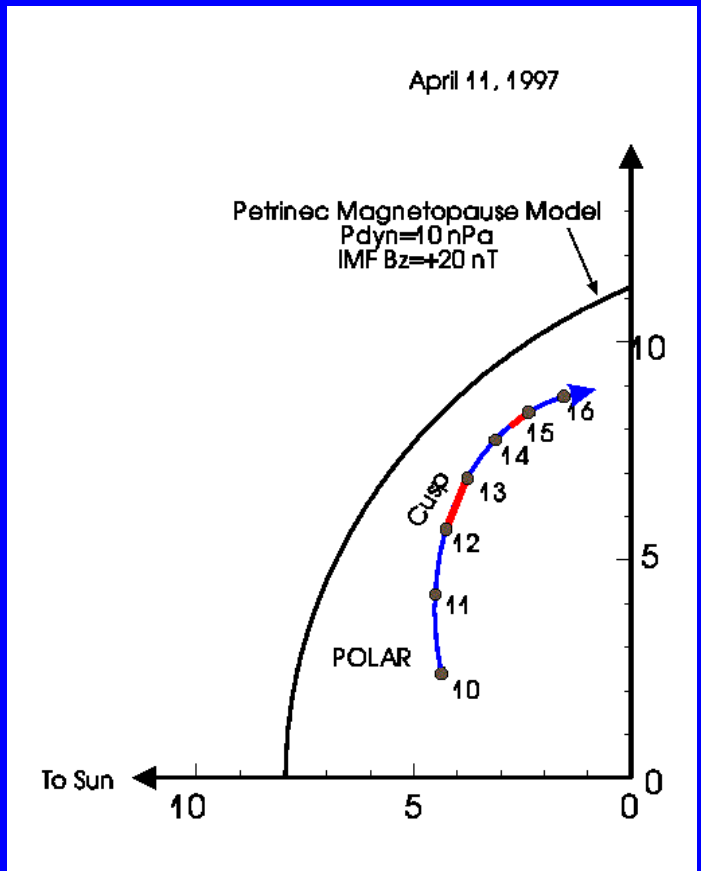
April 11, 1997
Petrinec Magnetopause Model
Pdyn=10 nPa
IMF Bz=+20 nT
Cusp
POLAR
16
15
14
13
12
11
10
To Sun
10
5
0
10
5
0

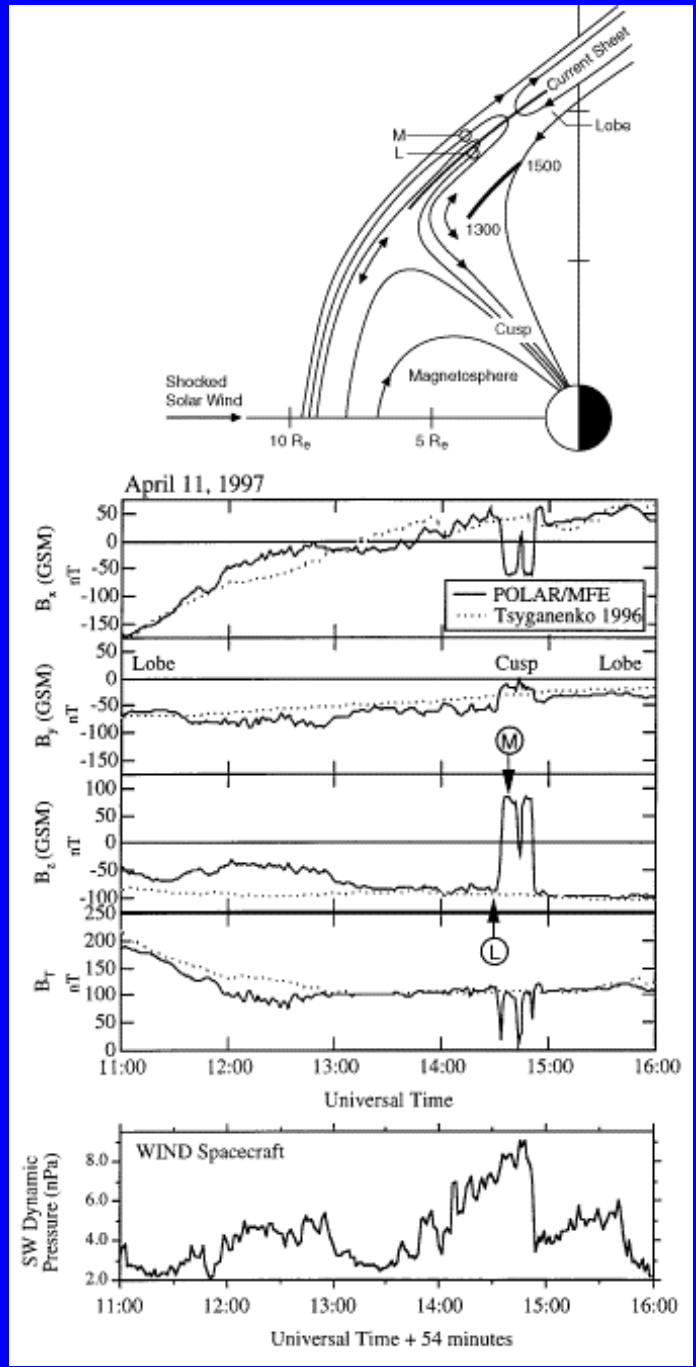
Current Sheet
Lobe
M
L
1500
1300
Cusp
Magnetosphere
Shocked
Solar Wind
10 Re
5 Re
April 11, 1997
Bx (GSM) nT
POLAR/MFE
Tsyganenko 1996
Lobe
Cusp
Lobe
By (GSM) nT
M
Bz (GSM) nT
L
BT nT
11:00
12:00
13:00
14:00
15:00
16:00
Universal Time
WIND Spacecraft
SW Dynamic Pressure (nPa)
Universal Time + 54 minutes

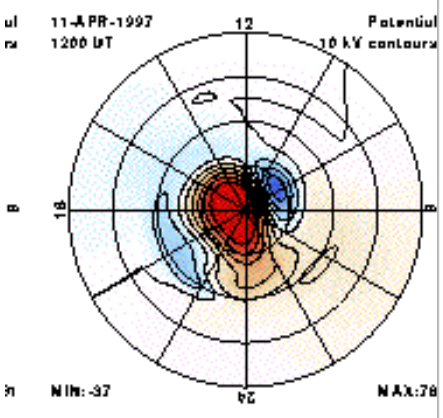
11-APR-1997
1200 UT
Potential
10 kV contours
12
18
24
Min: -37
Max: 78

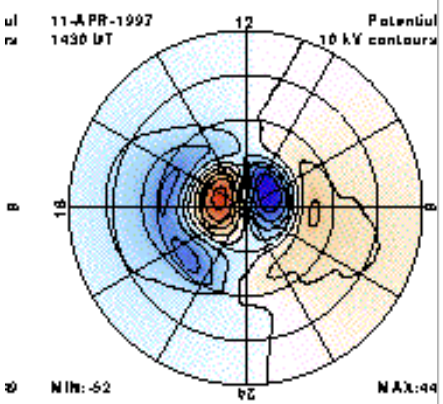
11-APR-1997
1430 UT
Potential
10 kV contours
12
18
24
Min: -62
Max: 44

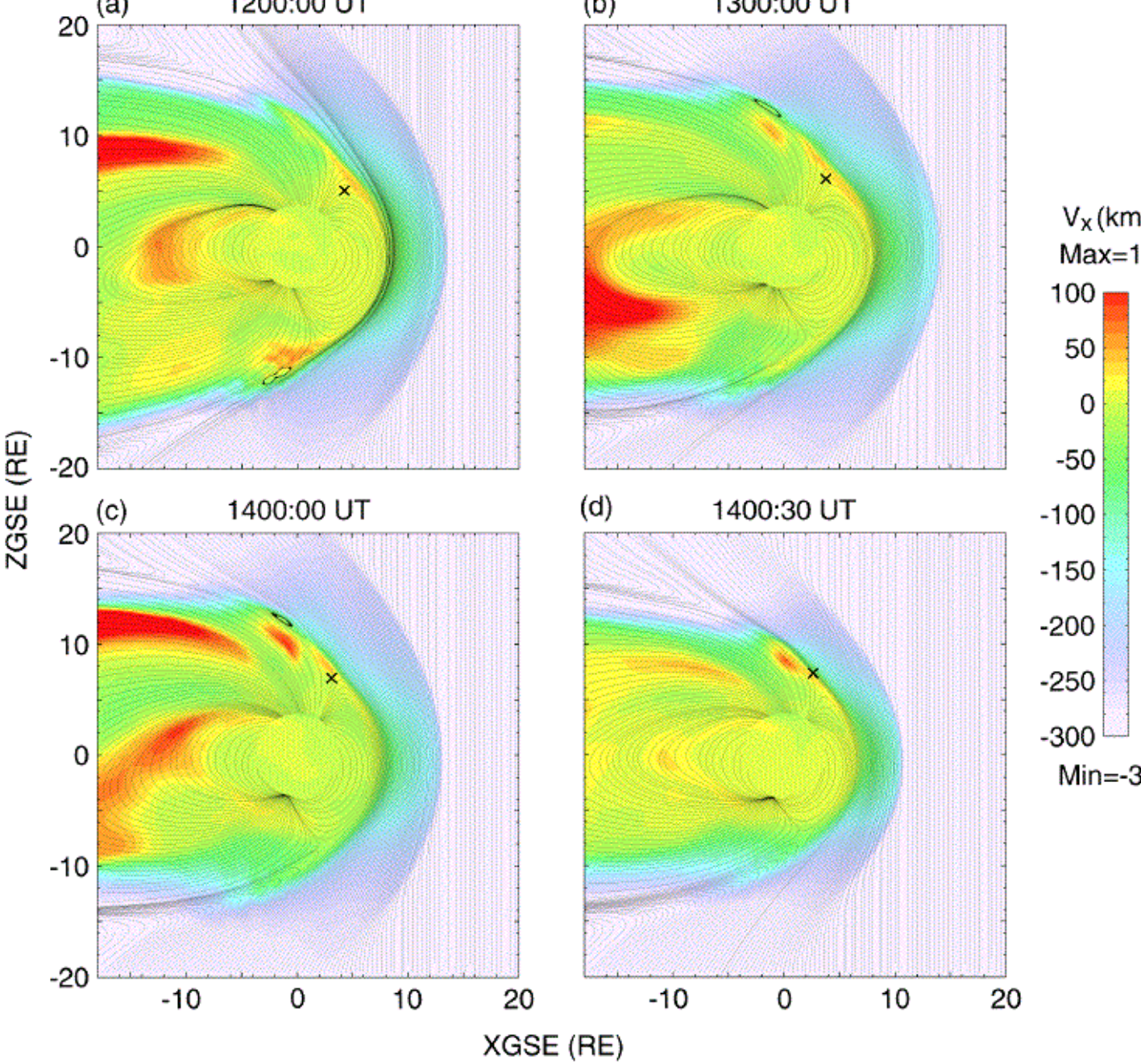
(a) 1200:00 UT
(b) 1300:00 UT
(c) 1400:00 UT
(d) 1400:30 UT
ZGSE (RE)
XGSE (RE)
20
10
0
-10
-20
V_X (km
Max=1
100
50
0
-50
-100
-150
-200
-250
-300
Min=-3

DATA:

Electric Field - **EFI** , F. S. Mozer, P.I., Univ. of Berkeley
Magnetic Field - **MFE**, C. T. Russell, P.I., UCLA
Plasma Data - **HYDRA**, J. S. Scudder, P.I., Univ. of Iowa
Energetic Particles - **CAMMICE**, T.A. Fritz, P.I., Boston University
Waves - **PWI**, D. Gurnett, P.I., Univ. of Iowa

Solar wind data - **WIND** and **GEOTAIL**

Solar wind conditions:

•April 11, 1997, 14:15-14:55 UT, magnetopause skimming due to a "valve" of enhanced p_{dyn}, at ~ [2.63,1.42, 8.08 , R_E] GSM, under solar wind with Mach numbers: [M_s, M_{ms}, M_A] = [9.0, 4.1, 4.7*], and a steady IMF= [3,-2, **20**] nT, GSM

The plasma depletion/magnetic flux pile-up layer formed itself in the magnetosheath just upstream the magnetopause and the MS flow stagnated to ~sub-Alfvénic velocities.

HYDRA spectrograms for April 11, 1997 high-latitude MP crossing

"B" - "bubble layer", magnetopause region with very depressed magnetic field,
"MS" - magnetosheath, PDL, magnetic flux pile-up (from Stasiewicz et al., 2002)

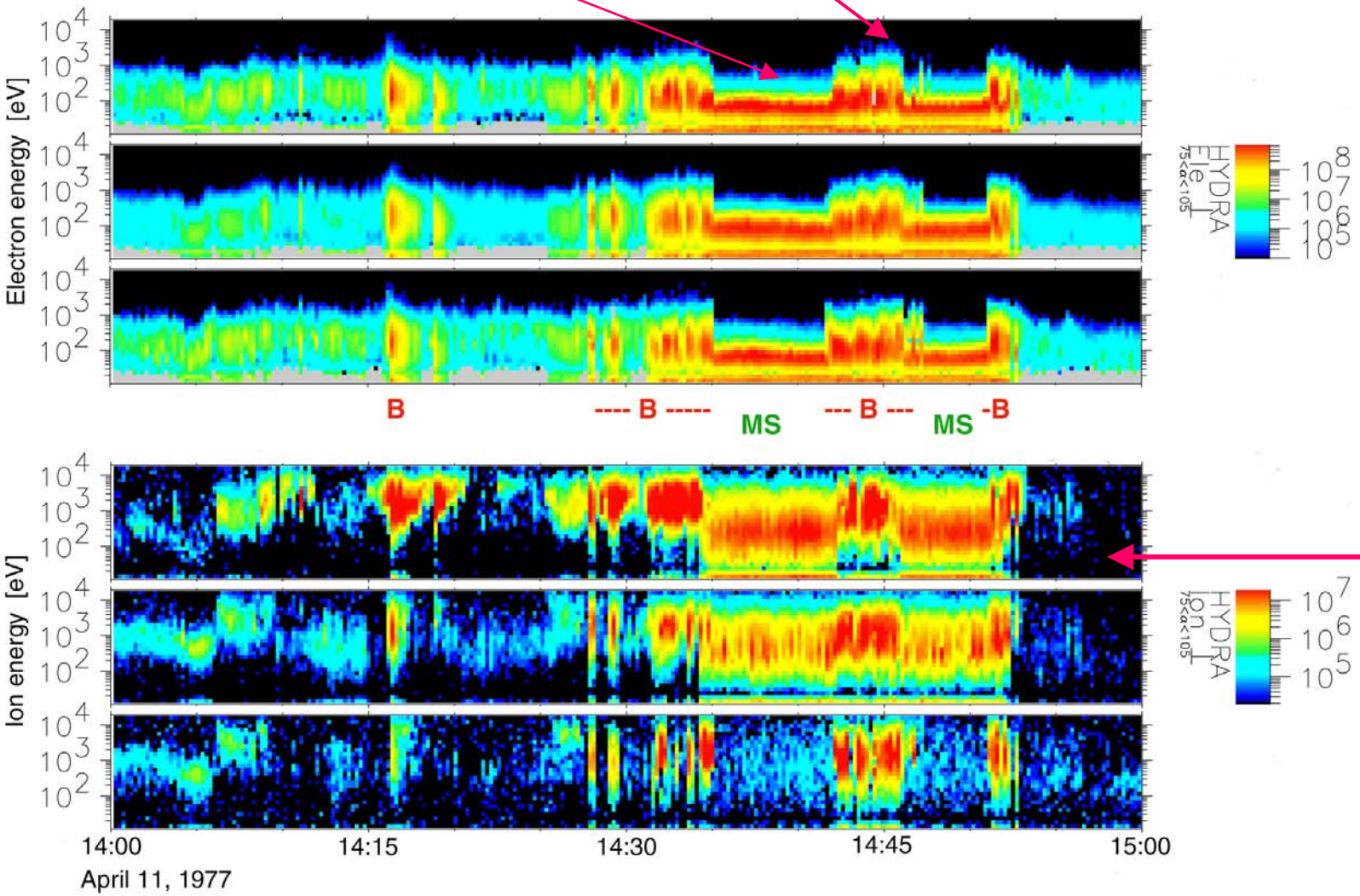

lobe

electrons, 0º, 90º, 180º p.a.

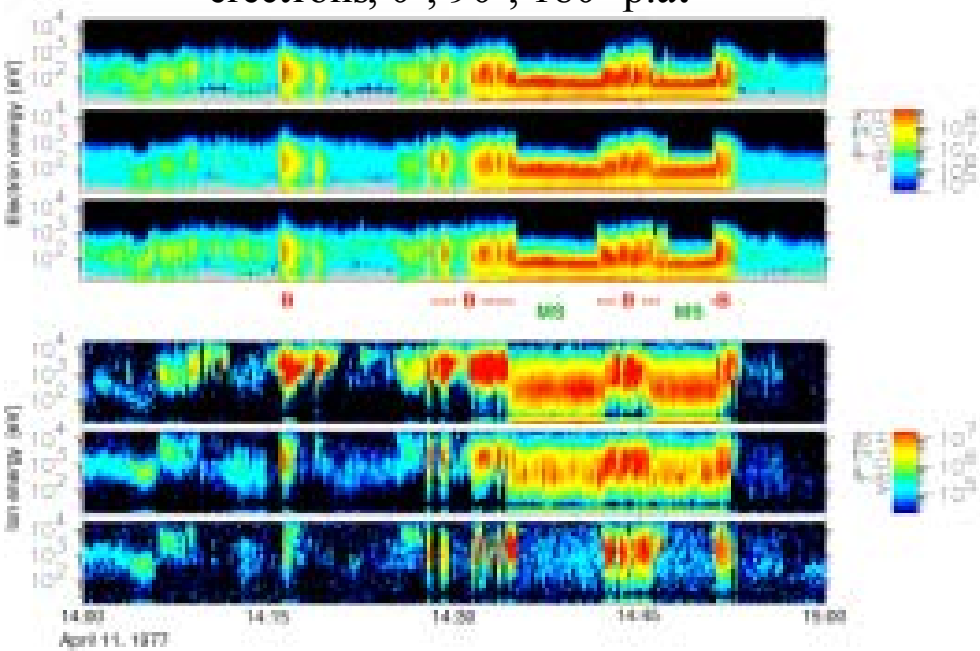

ions , 0º, 90º, 180º p.a.

HYDRA spectrograms

Fig. 1

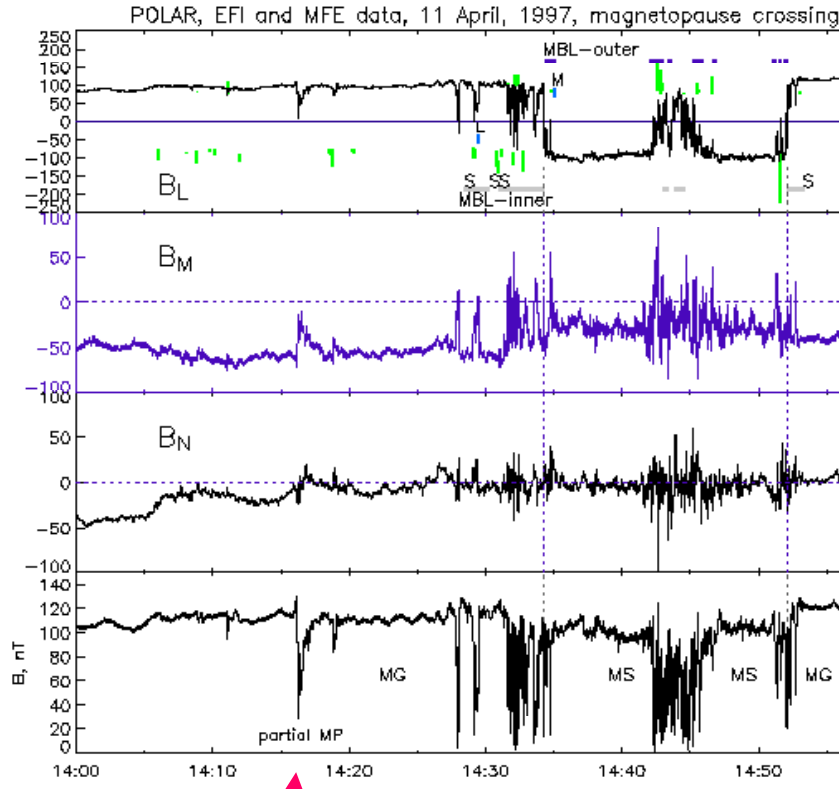

MFE, magnetic field in LMN coordina

Fig. 2

First approach to MP

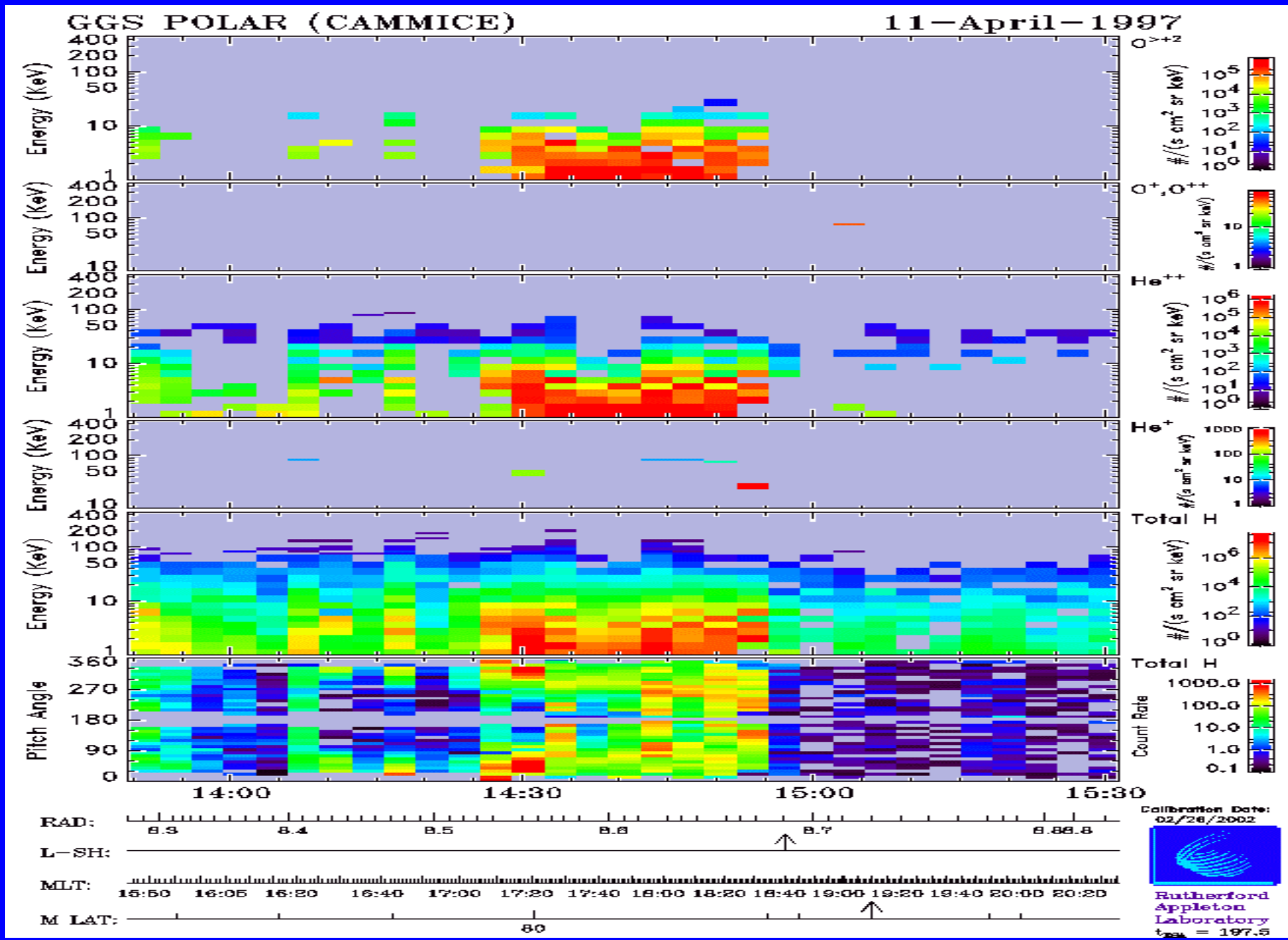
GGS POLAR (CAMMICE)
11-April-1997
Energy (KeV)
Pitch Angle
O>+2
O+,O++
He++
He+
Total H
Count Rate
#/(s cm2 sr keV)
14:00
14:30
15:00
15:30
RAD:
L-SH:
MLT:
M LAT:
Calibration Date:
02/26/2002
Rutherford
Appleton
Laboratory

Magnetic structure:

- The magnetic shear is ~150 degrees, so there is a guide field as large as ~25% of the MS magnetic field.
- ***Figure 2*** shows many full crossings of the magnetopause current layer, as well as several partial magnetopause crossings.
- Each full or partial MP crossing features of deep depression of B.
- The hodograms of full crossings have different shapes, from oval shaped to S-shaped, with only one crossing featuring a semi-circular rotation.
- ***Figure 4*** shows examples of hodograms. Deepest depressions correspond to S-shape hodograms, that accompany most sudden transitions, with 2-s for the complete transition from MG-like to MS-like magnetic field. The distribution of depth and half-thickness of depression "wall" for all transitions and those with S-shaped hodograms is shown next .

Examples of hodograms across the MP current layer

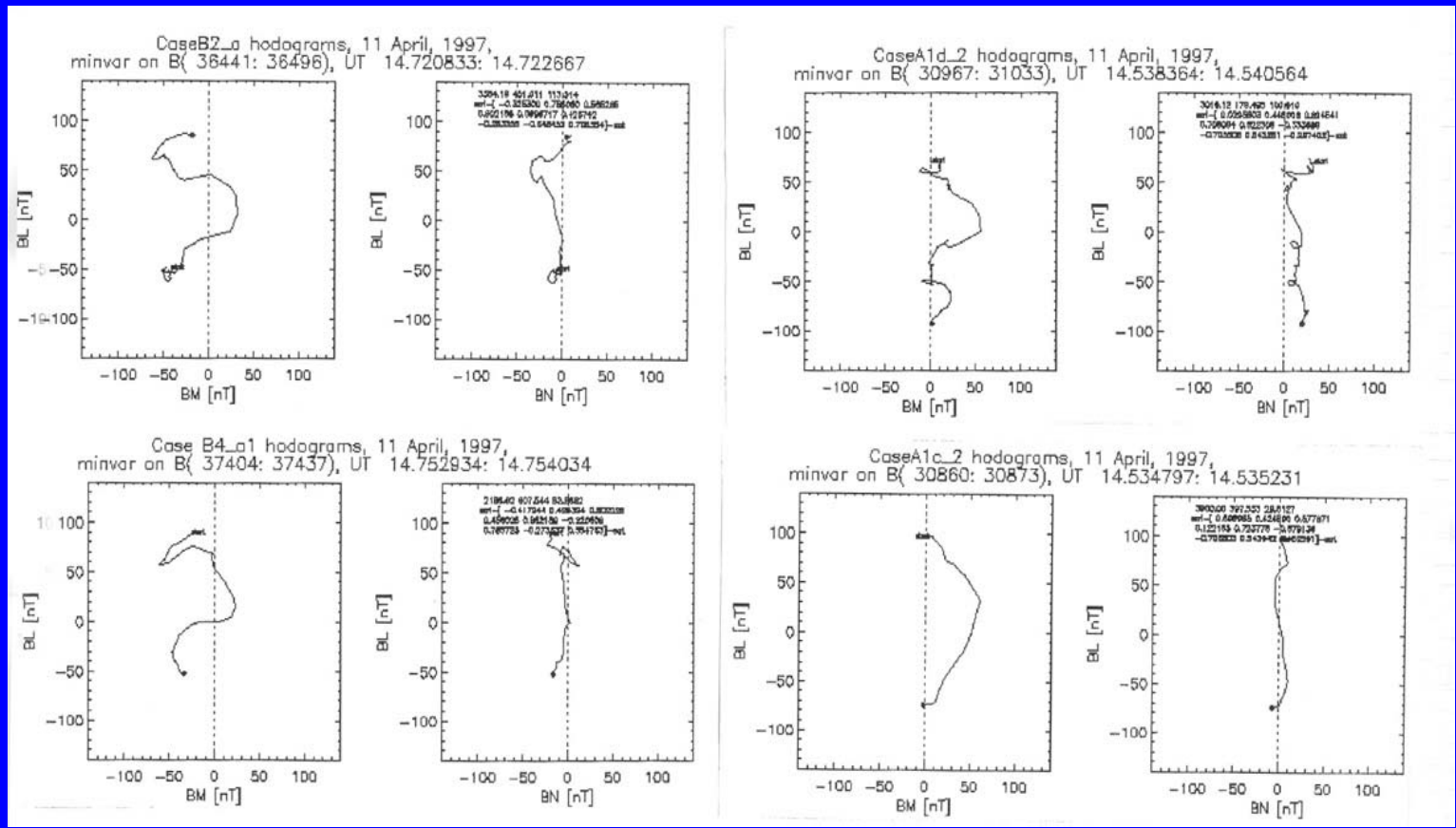

Assuming $V_{MP,n}$ **=50 km/s to 100 km**/s, the half-thickness of the „wall" of magnetic cavity within the field reversal region is 50 to ~ 100 **km** for half of all MP crossings, and **30 to ~60 km** for half of those with **S-shaped hodograms**. This is to be compared with MS ion Larmor radius $\mathbf{r_{i,L}}$ **= 50 km** (for $v_{i,th}$), and MS ion inertial length $\mathbf{d_i}$ **=~15 km**, in the plasma depletion layer just upstream of MP.

All MP

S-shaped

POLAR, MFE data, magnetopause on April 11, 1997
main current layer (MP), all type of hodograms

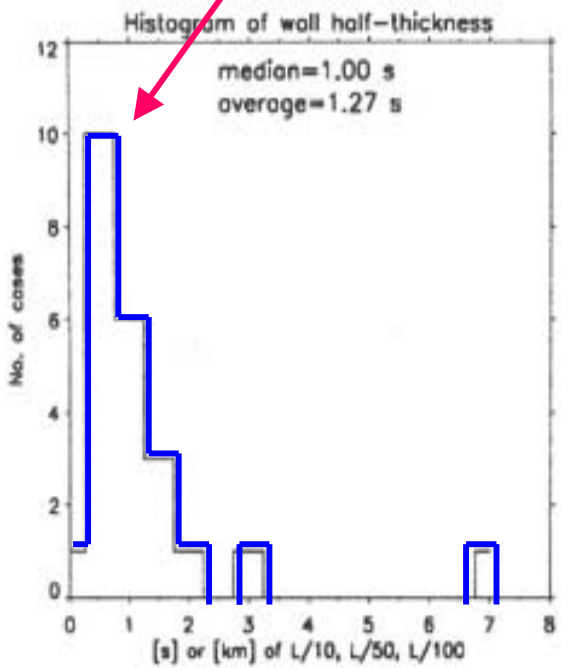

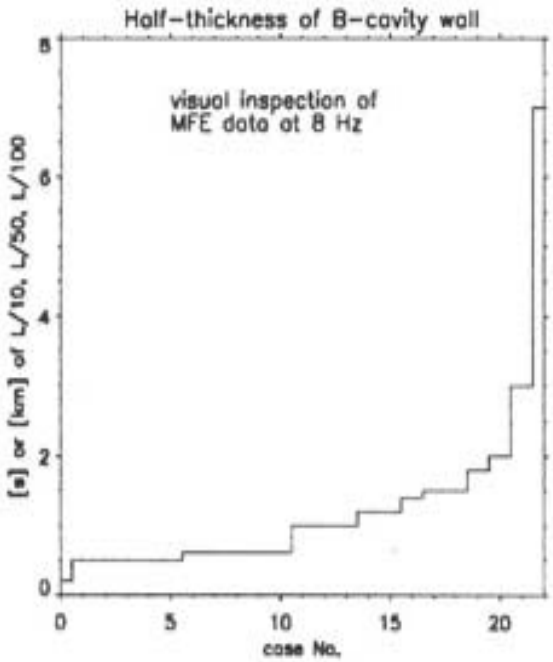

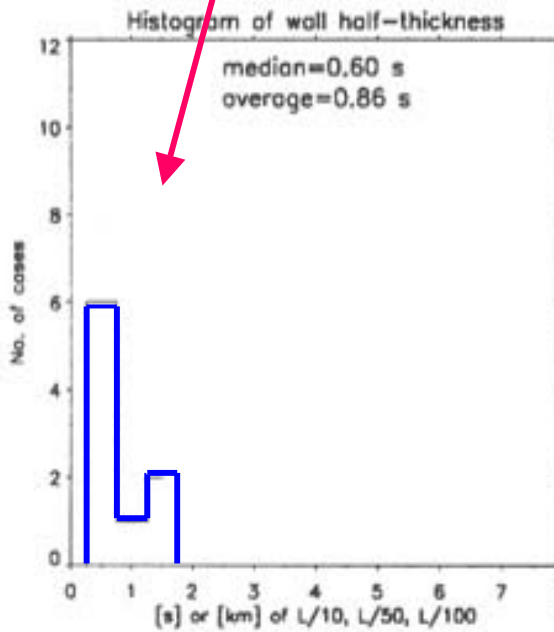

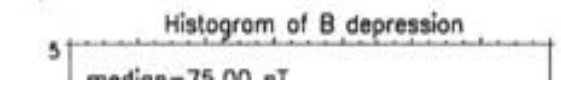

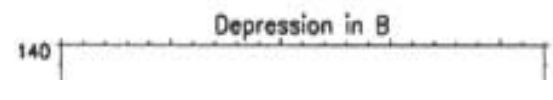

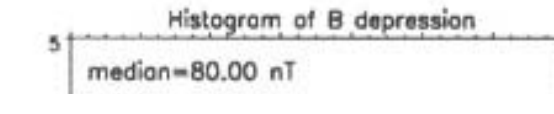

Plasma waves:

- Magnetopause crossings typically are accompanied by strong wave activity in wide frequency range. ***Figures 6 a,b*** show wave spectrograms from Step Frequency Receiver of PWI , for magnetic and electric wave component. Detailed analysis shows that in the magnetopause boundary layers close to MP the dominating wave modes change rapidly on milisecond time scale, especially in the case of thin current sheet, as is the case here.

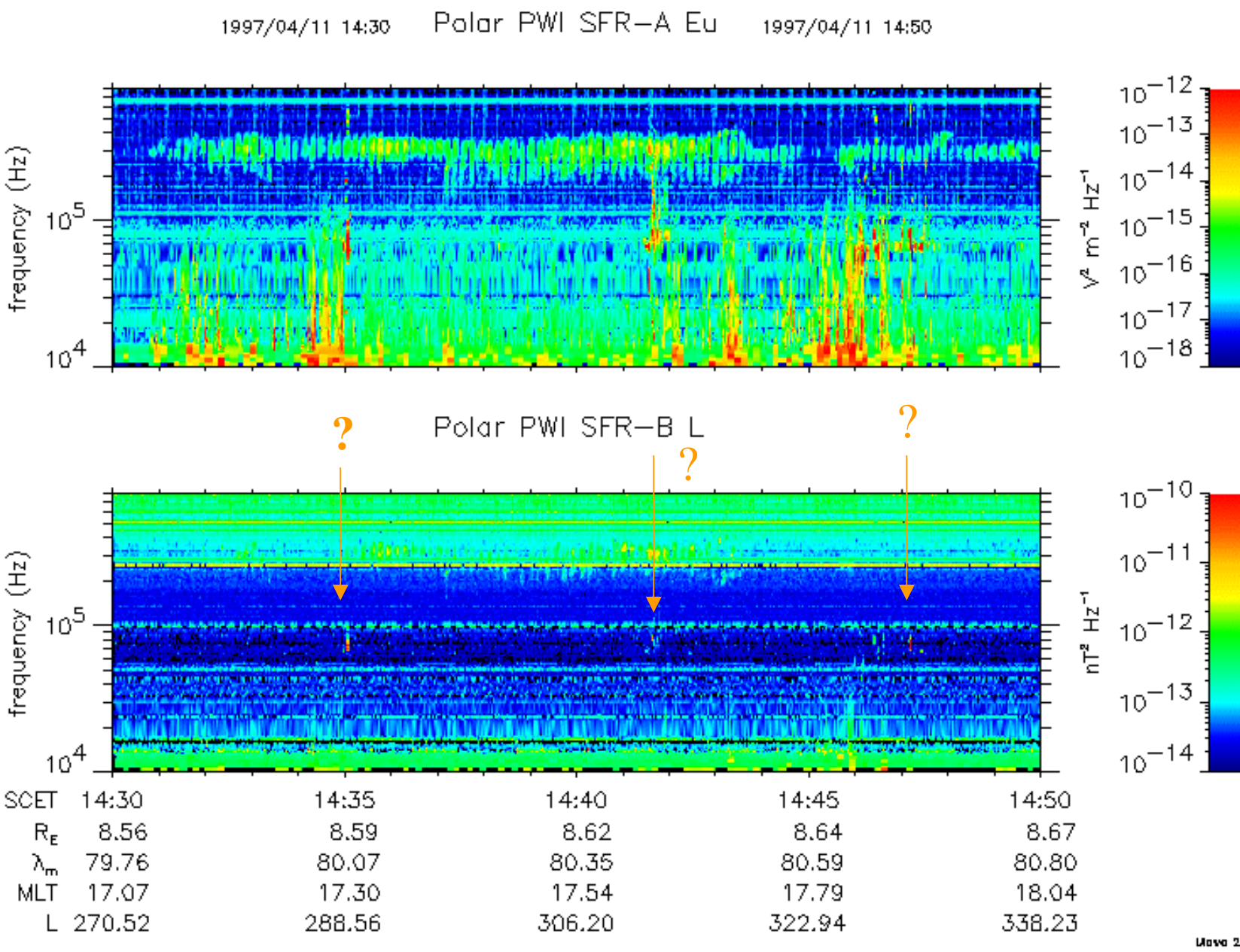
1997/04/11 14:30
Polar PWI SFR–A Eu
1997/04/11 14:50
frequency (Hz)
10^5
10^4
$V^2\ m^{-2}\ Hz^{-1}$
10^{-12}
10^{-13}
10^{-14}
10^{-15}
10^{-16}
10^{-17}
10^{-18}
?
?
?
Polar PWI SFR–B L
frequency (Hz)
10^5
10^4
$nT^2\ Hz^{-1}$
10^{-10}
10^{-11}
10^{-12}
10^{-13}
10^{-14}
SCET 14:30 14:35 14:40 14:45 14:50
R_E 8.56 8.59 8.62 8.64 8.67
λ_m 79.76 80.07 80.35 80.59 80.80
MLT 17.07 17.30 17.54 17.79 18.04
L 270.52 288.56 306.20 322.94 338.23

Partial MP crossing at 14:16:00 UT

- EFI was triggered in burst mode during this uncompleted MP crossing. ***Figure 7*** shows summary of observed field and wave structures. Local compression of the magnetic field with the accompanying depression of plasma density at the separatrix was the site of intense lower hybrid wave turbulence, as predicted, e.g., by *Shay et al., 2001* numerical simulation of reconnection (with 2 1/2 D electron particle-in-cell code). ***Figure 8*** shows wavelet spectrogram of LH turbulence at the separatrix (EFI 1600 Hz data) and ***Figure 9*** shows the same for the whistler waves in the depressed B-field region (PWI search coil data). ***Figure 10 a,b*** is the example of electron holes found at the wall and within the B-depression region, as recorded by WBR of PWI.

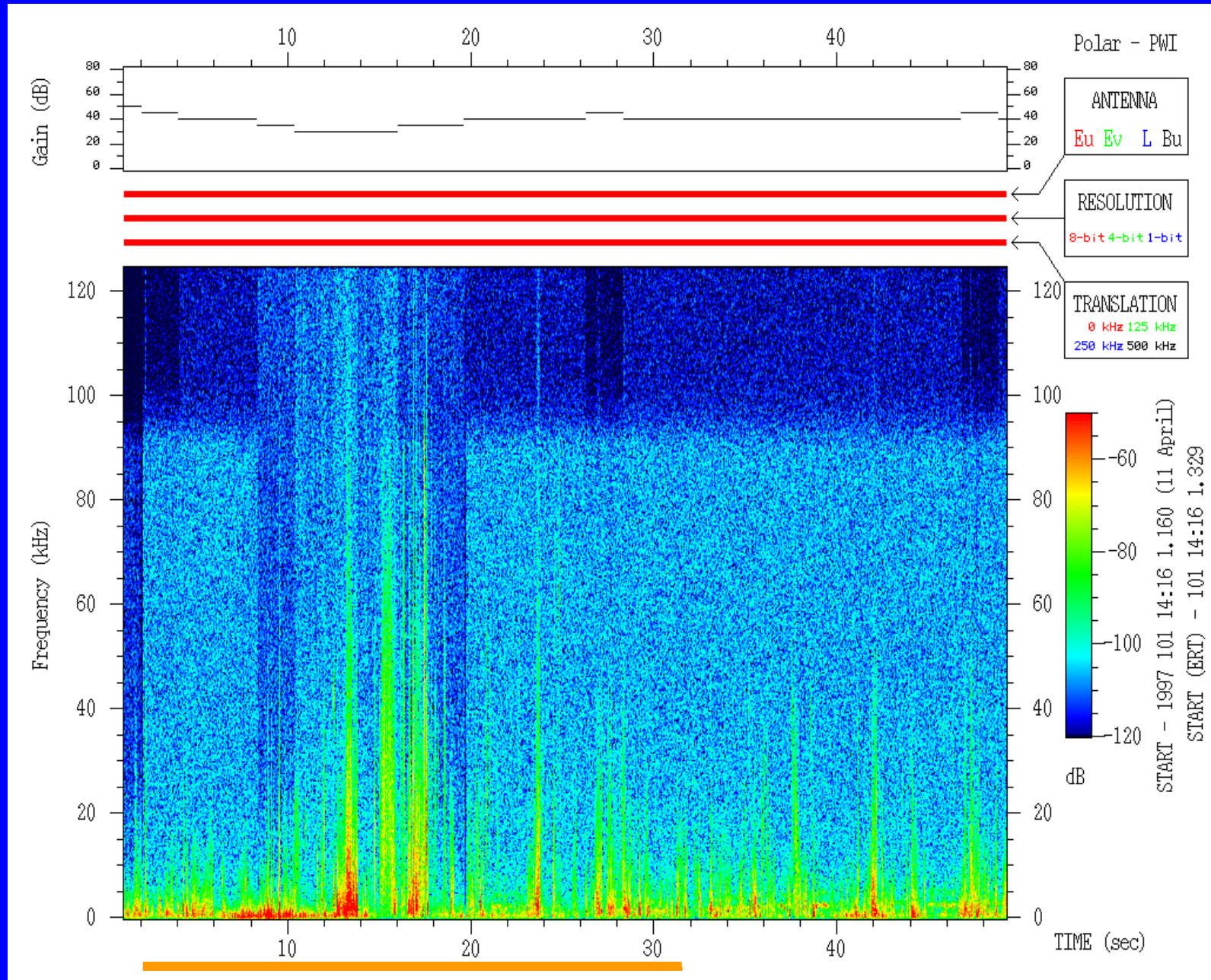

EFI burst mode

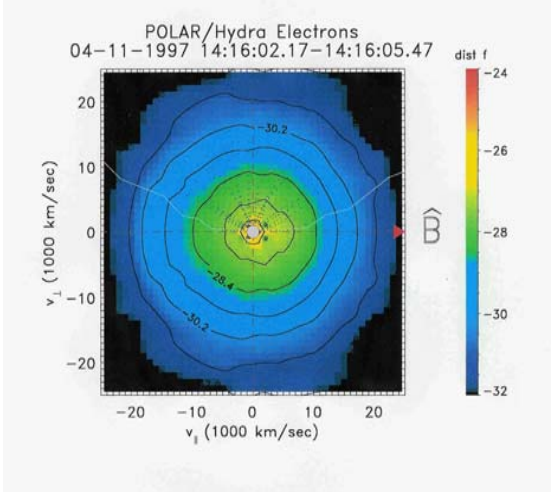

S1

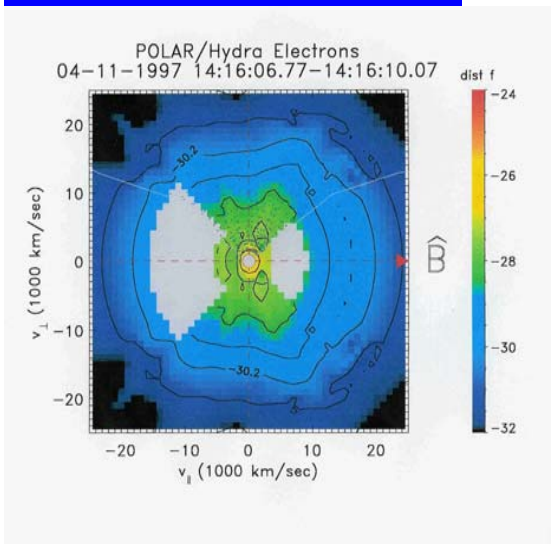

S2

Polar, partial MP crossing
MFE, magnetic field
EFI, spacecraft potential, burst mode

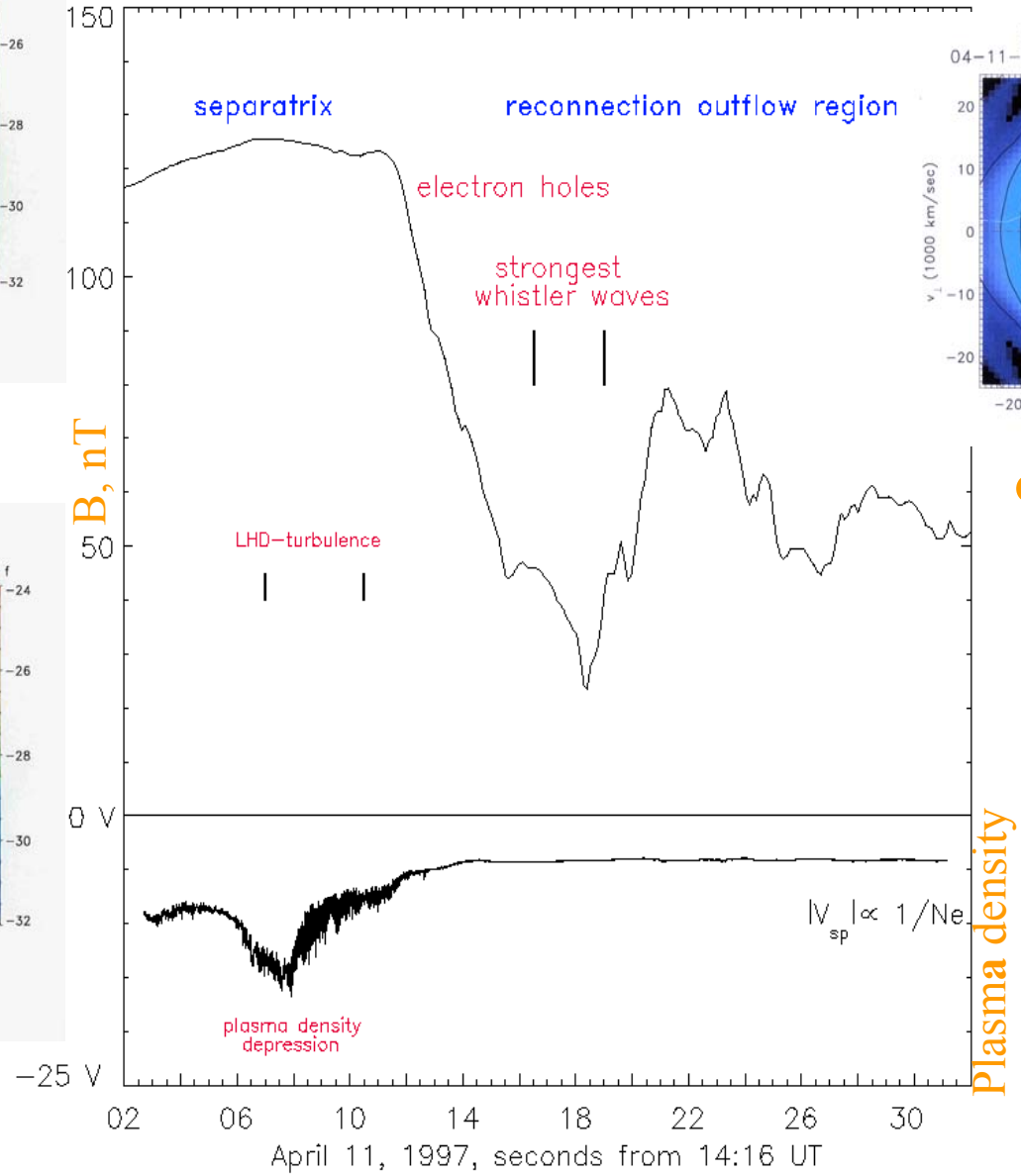

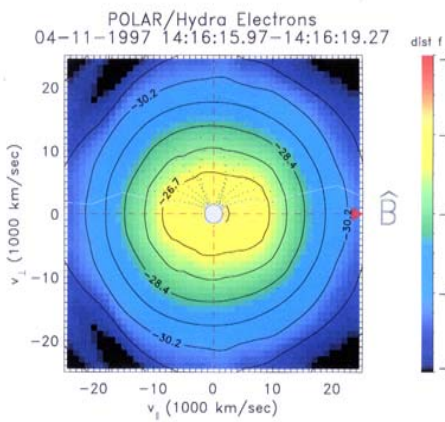

outflow region,
O

Wavelet spectrogram of LH waves at the separatrix

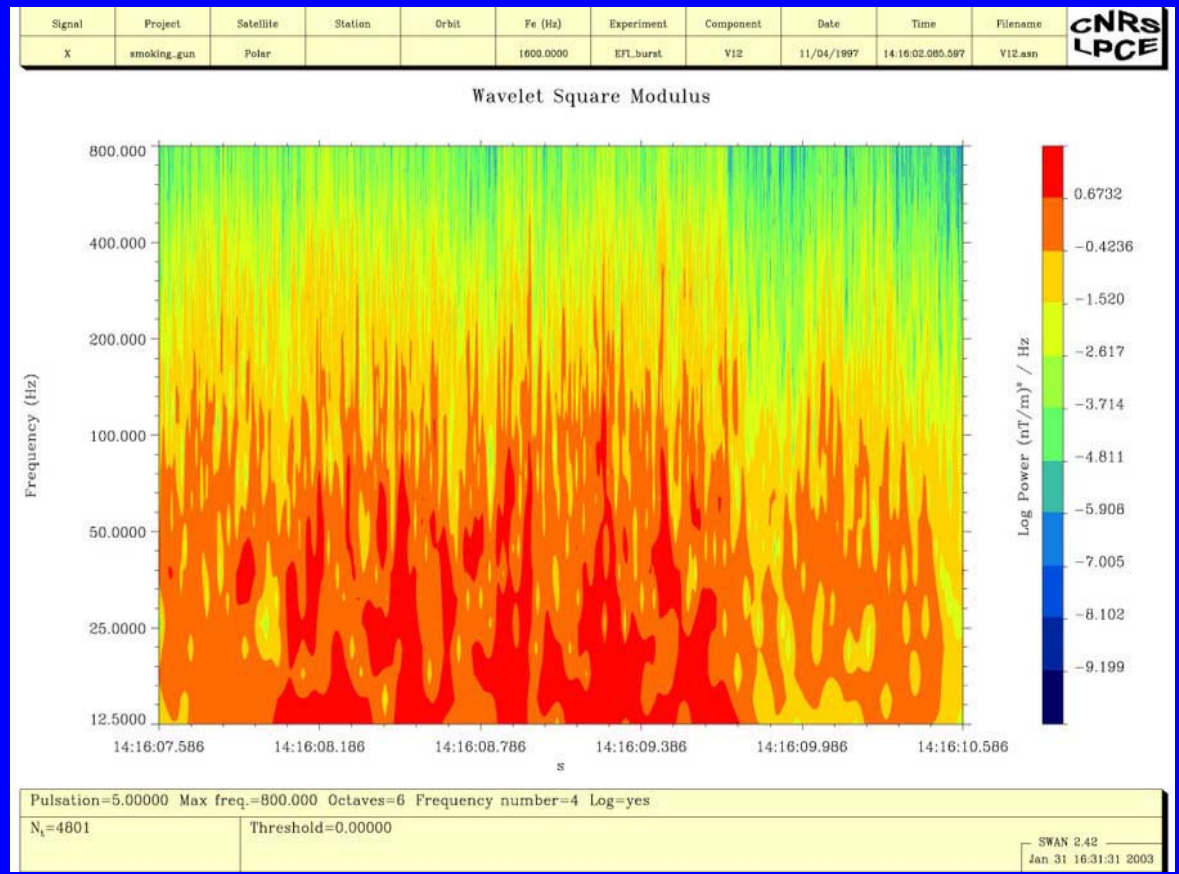

Wavelet spectrogram of whistler packets

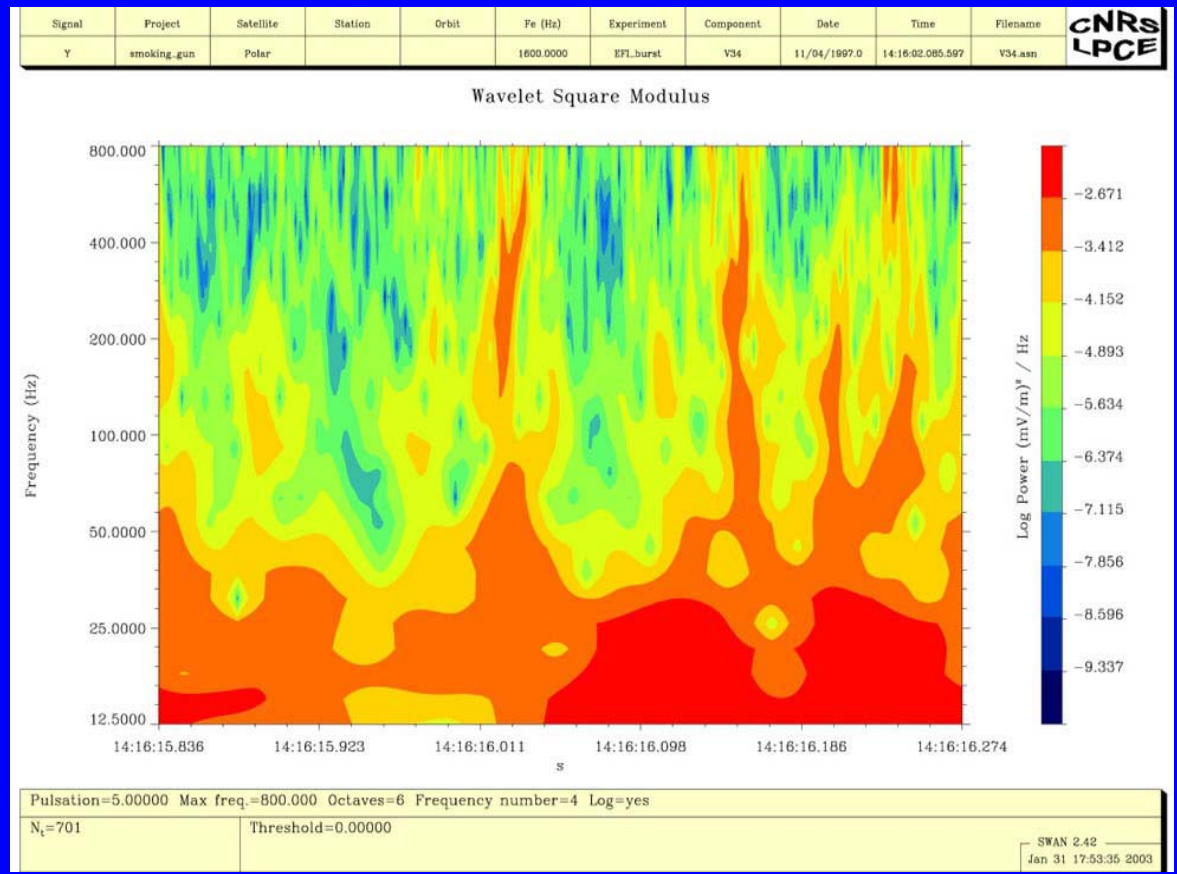

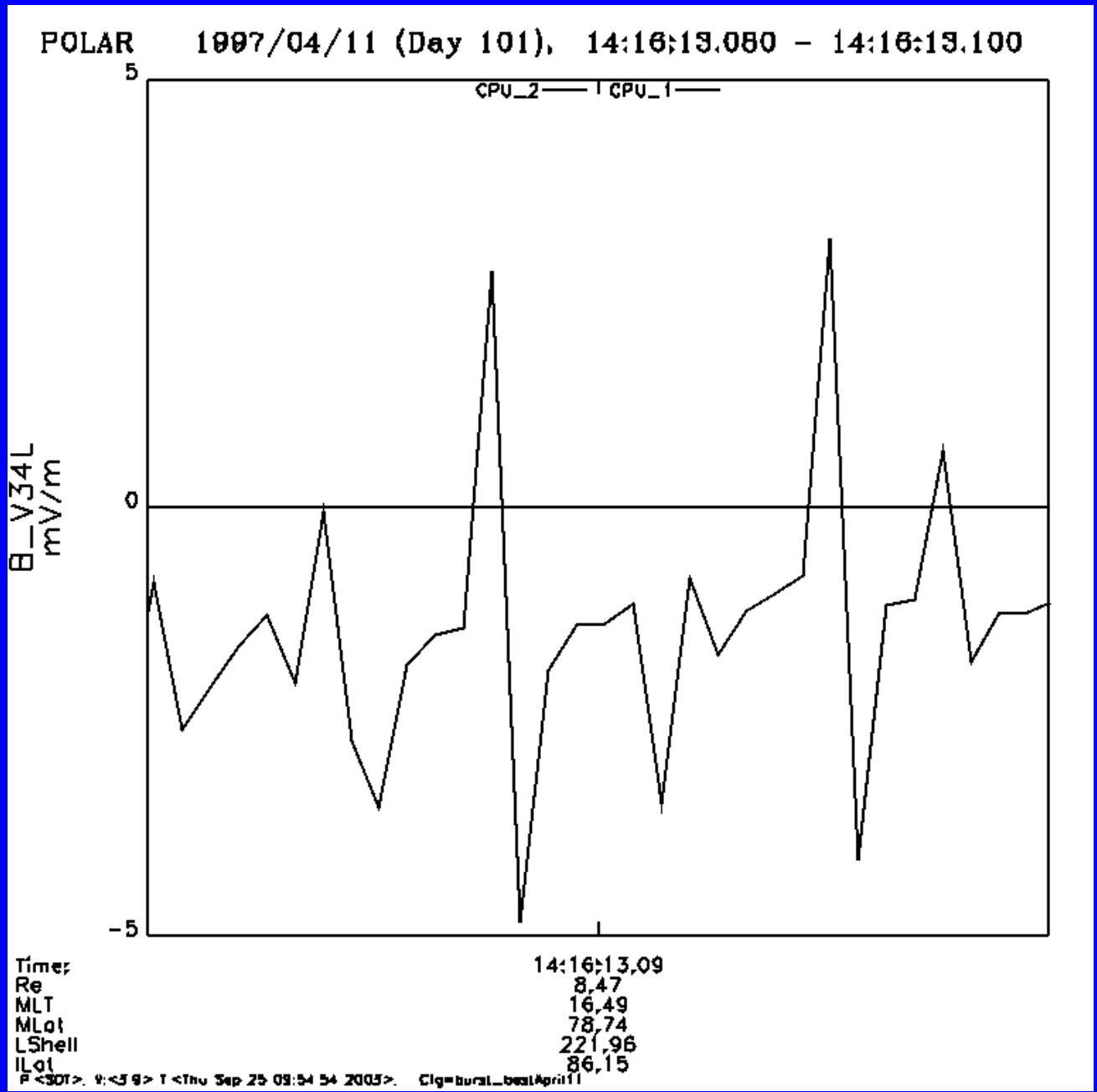
POLAR 1997/04/11 (Day 101), 14:16:13.080 - 14:16:13.100
CPU_2
CPU_1
5
0
-5
B_V34L
mV/m
Time:
Re
MLT
MLat
LShell
ILat
14:16:13.09
8.47
16.49
78.74
221.96
86.15

Electron holes (electron solitary waves) in the reconnection outflow region

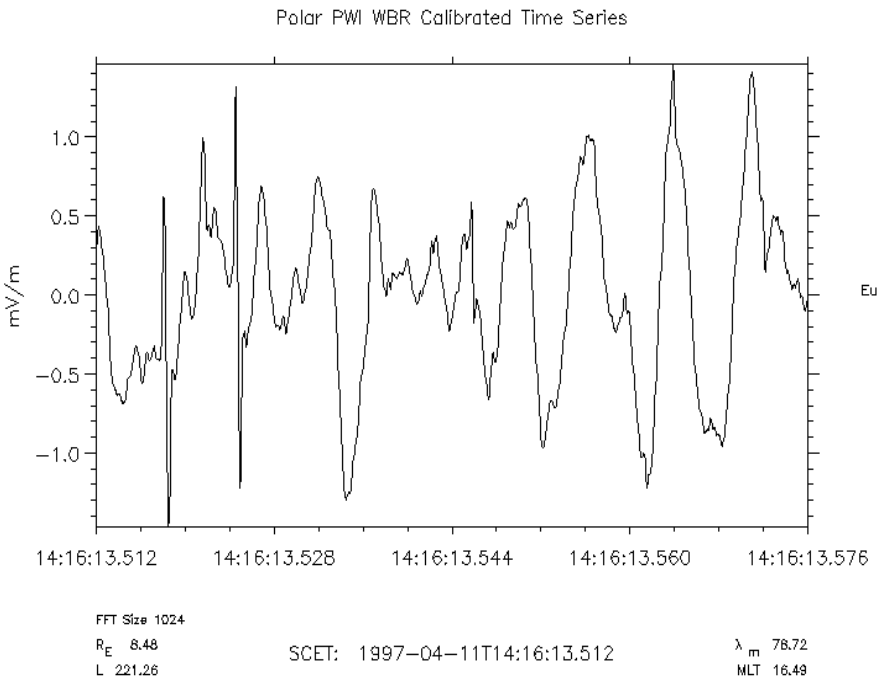

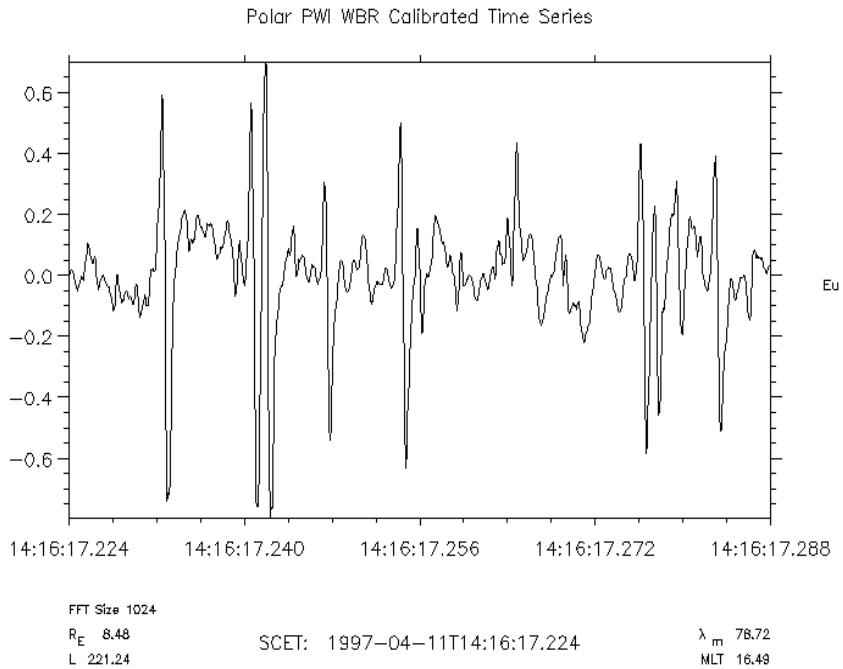

HYDRA electron distribution function $f(v_{perp},v_{par})$ at the „bottom" of magnetic cavity (obtained under the assumption of gyrotropy). Weak signatures of high-energy electron beam are seen at the edge of spectrogram high-energy cut-off (left side). Ion $f(v_{perp},v_{par})$ should be inspected, too (no ion data yet).

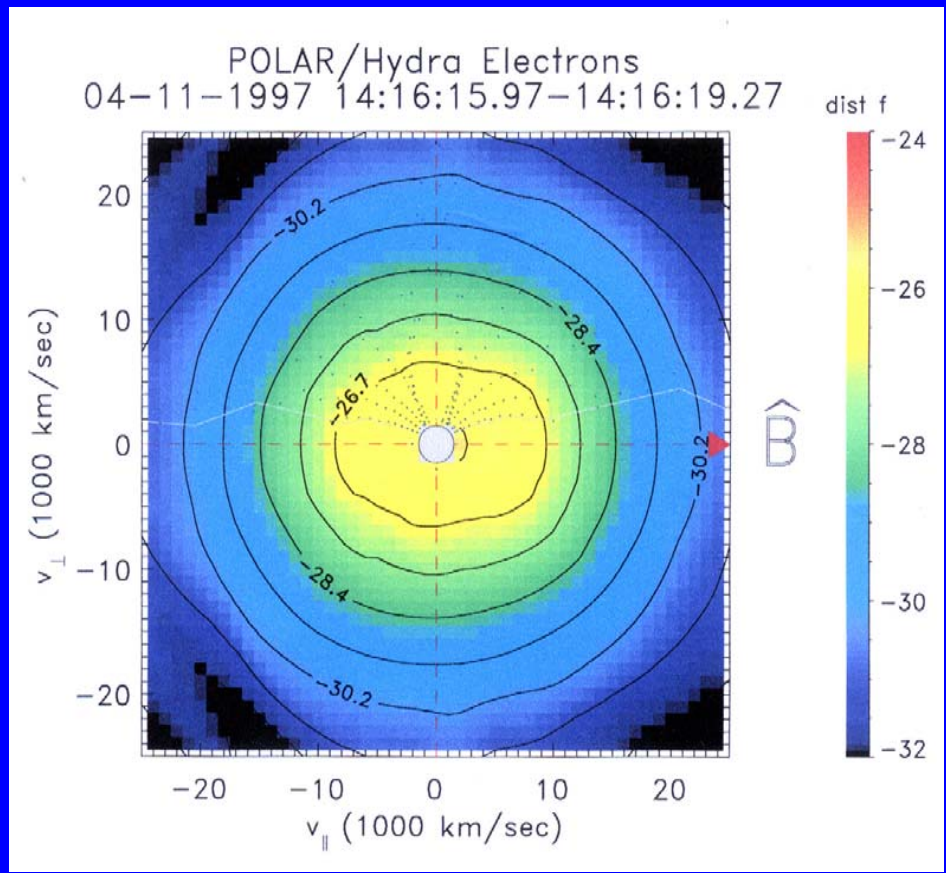

First completed MP crossing:

- HYDRA spectrograms for electrons and ions, skew and anisotropy of $f(v_{\perp}, v_{||})$
- B in LMN coordinates

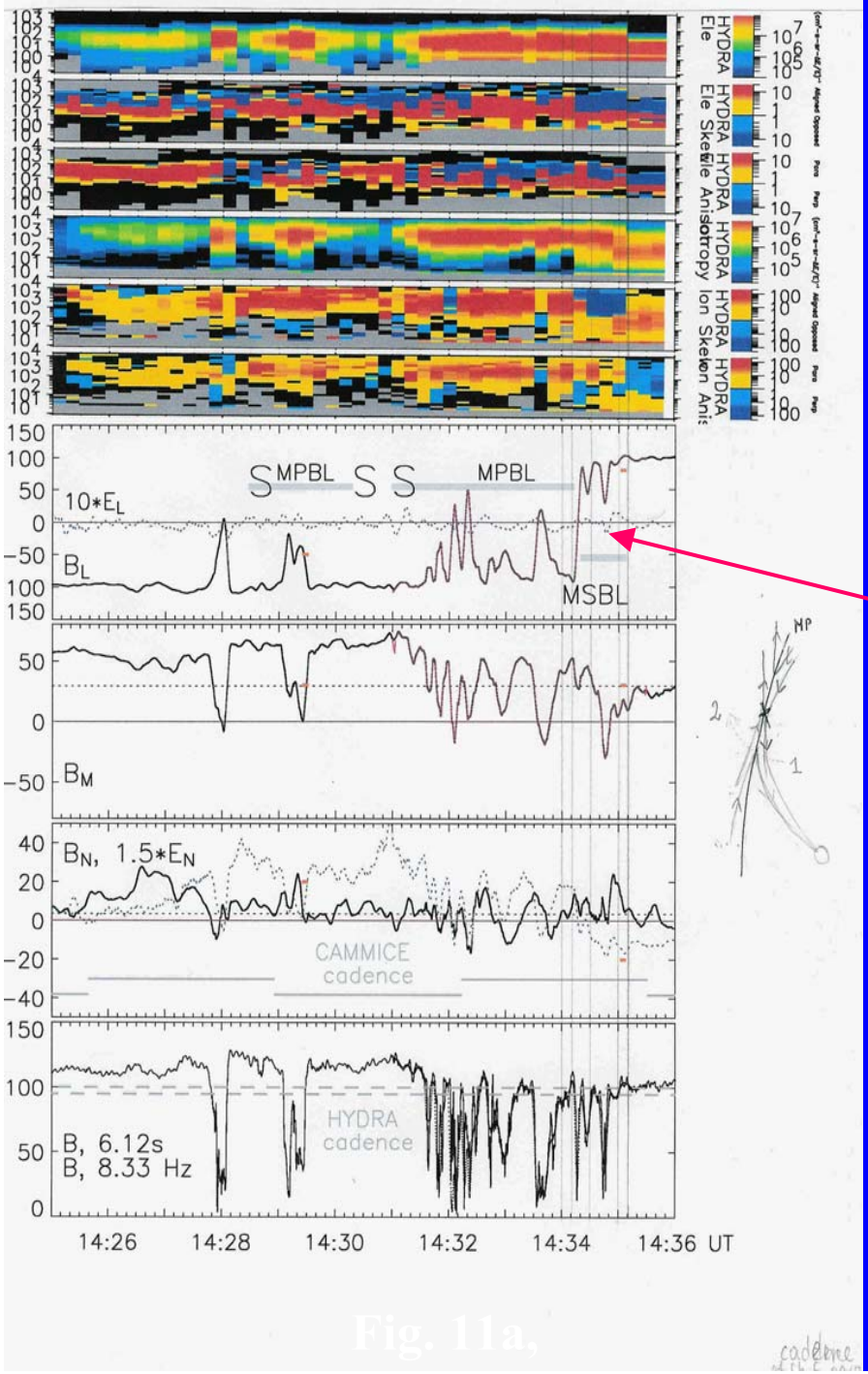

Fig. 11a,

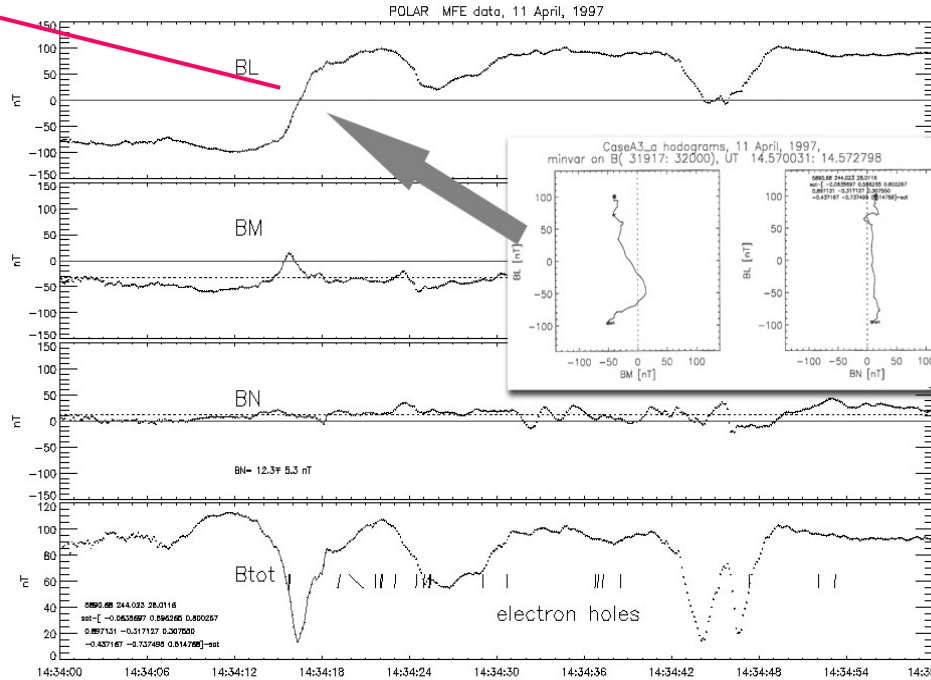

- electron solitary waves in the reconnection outflow region:

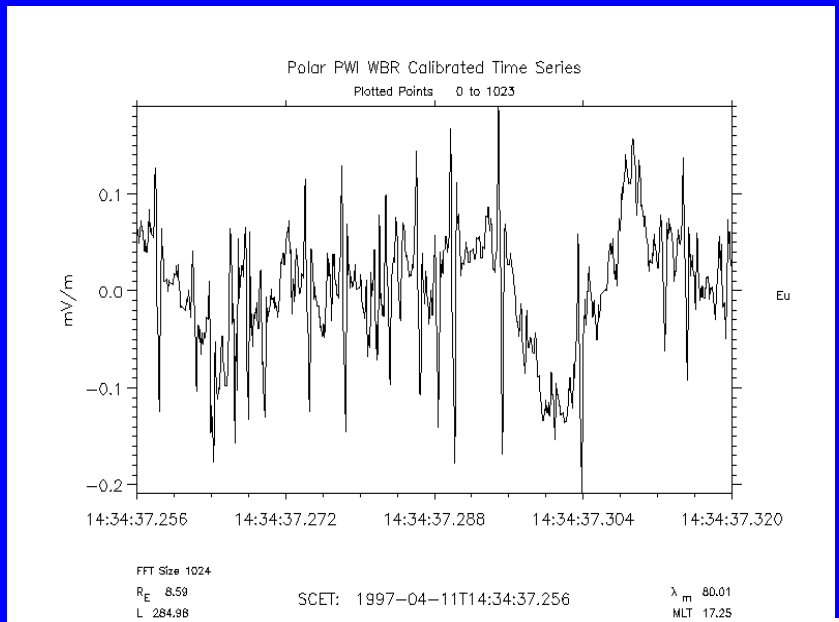

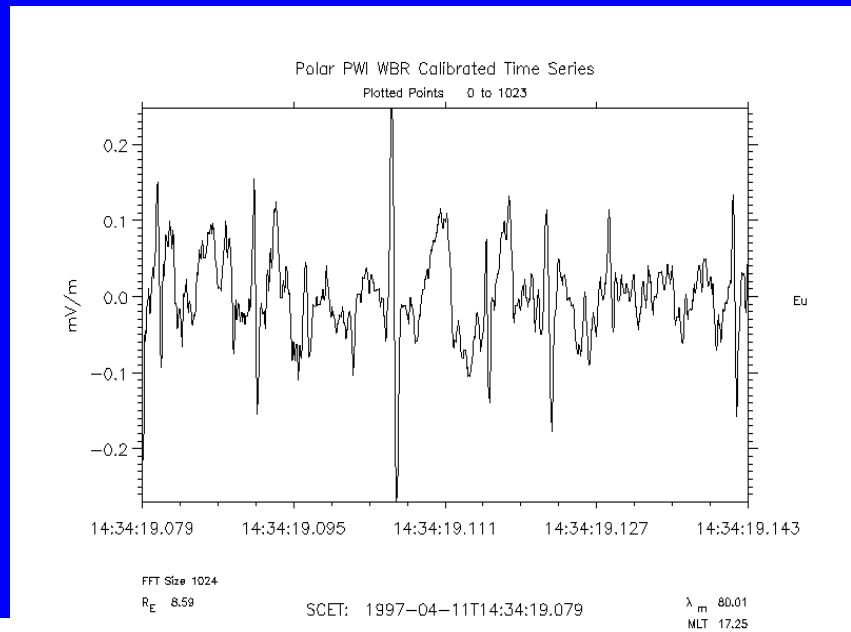

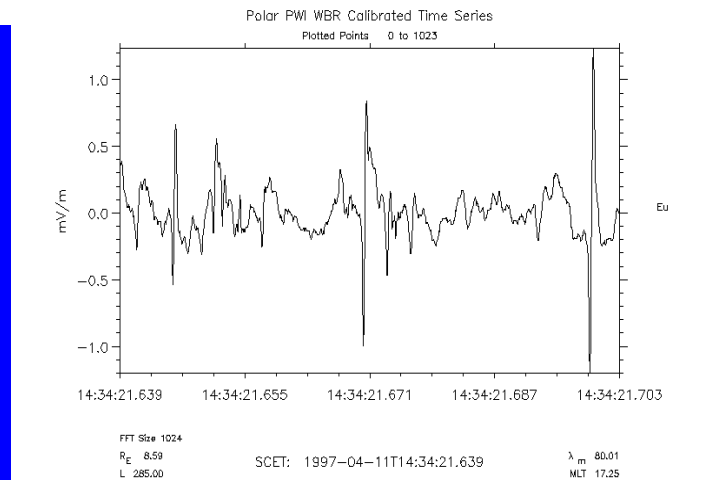

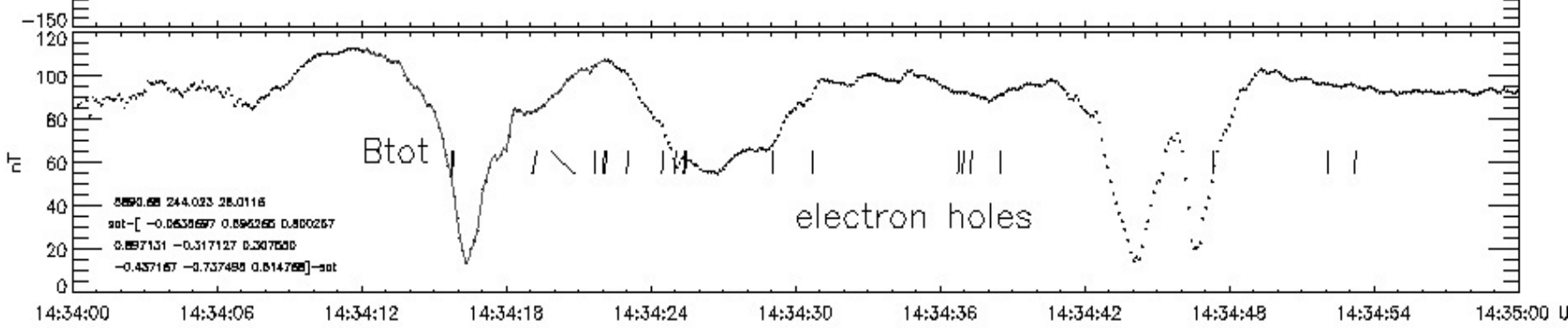

Regions where electron solitary waves were observed are marked with strips on B-panel.
WBR waveform however are not obtained continuously.

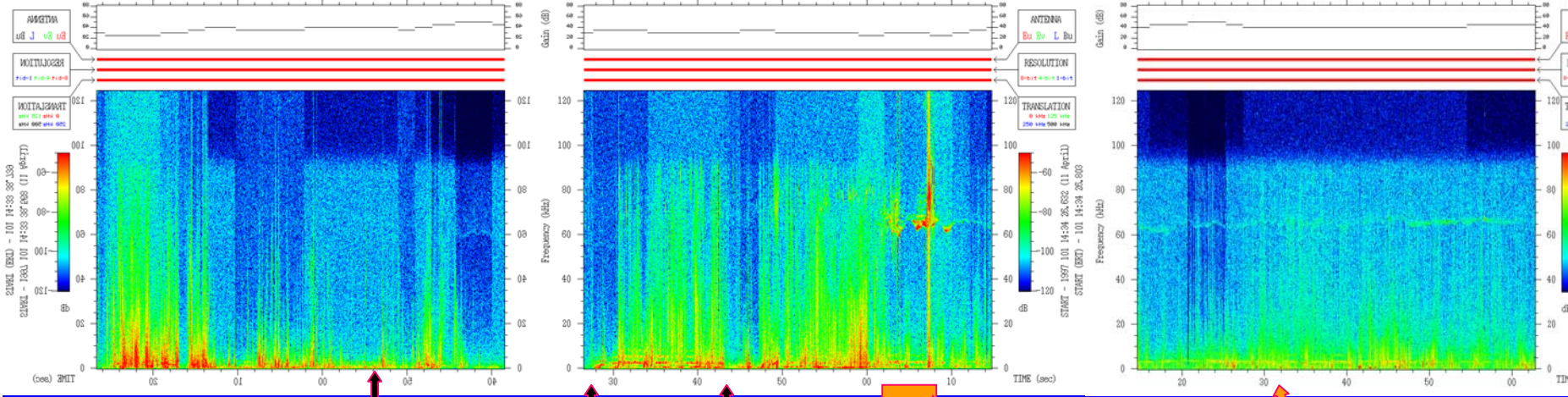

MP/CS center & B-cavity

B-cavities

"free flow " MS, PD

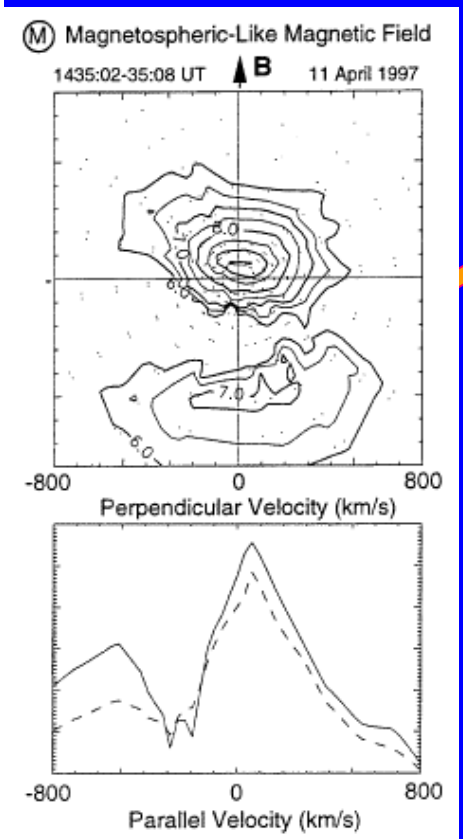

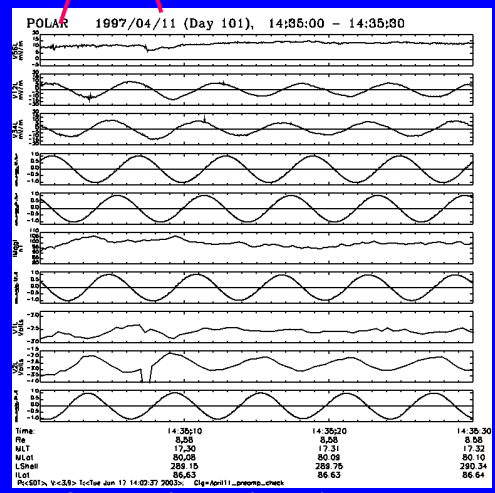

-TIMAS, ion distribution function in the MSBL (Fig. 4 of Russell et al., J. Geophys. Res., 105, 5489-5495, 2000) corresponding to Langmuir waves interval.

-Wide-band wave activity is supressed within magnetic cavities wherever B drops below some limit (e.g., electron holes are seen at cavity walls, but not at the "bottom").

MP_out,
event A

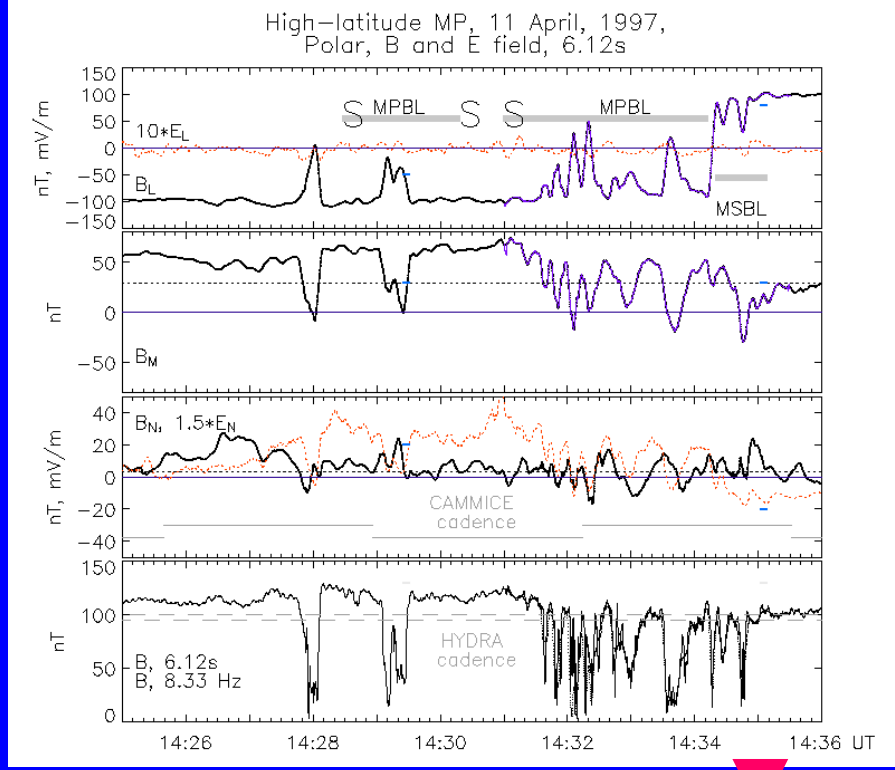

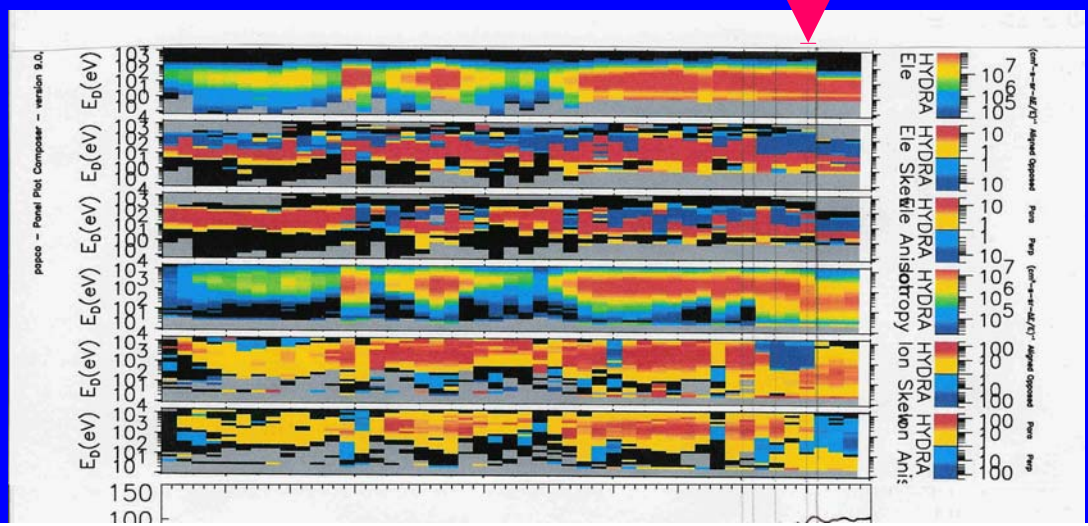

Arrow marks
the occurrence of
Langmuir waves.
They were observe
at the separatrix of
the reconnection
outflow region on t
MS side

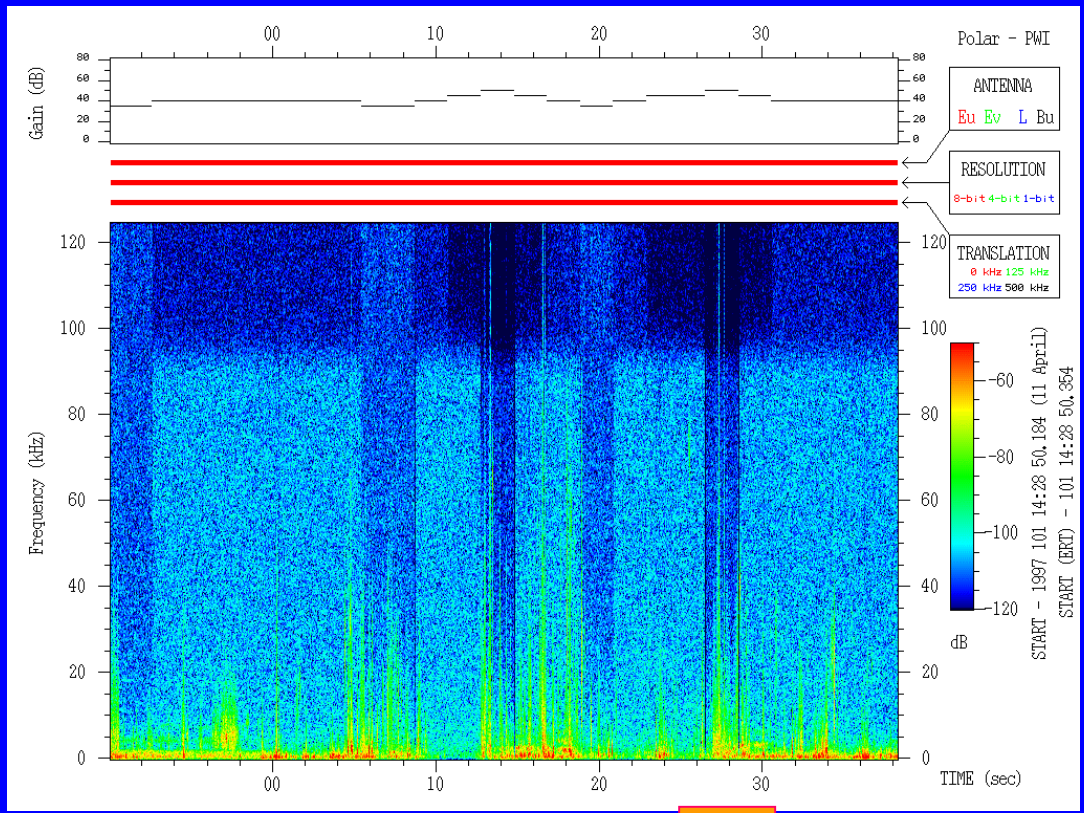

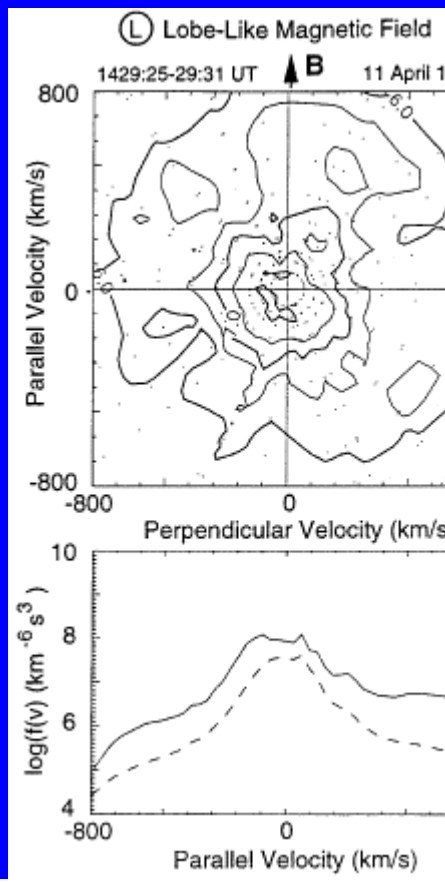

High-frequency waves are absent inside the magnetopause, as seen at this spectrogram for 14:29:50-14:30:38 UT.

First MP out, energetic ions

lobe

MPBL

MS, PDL

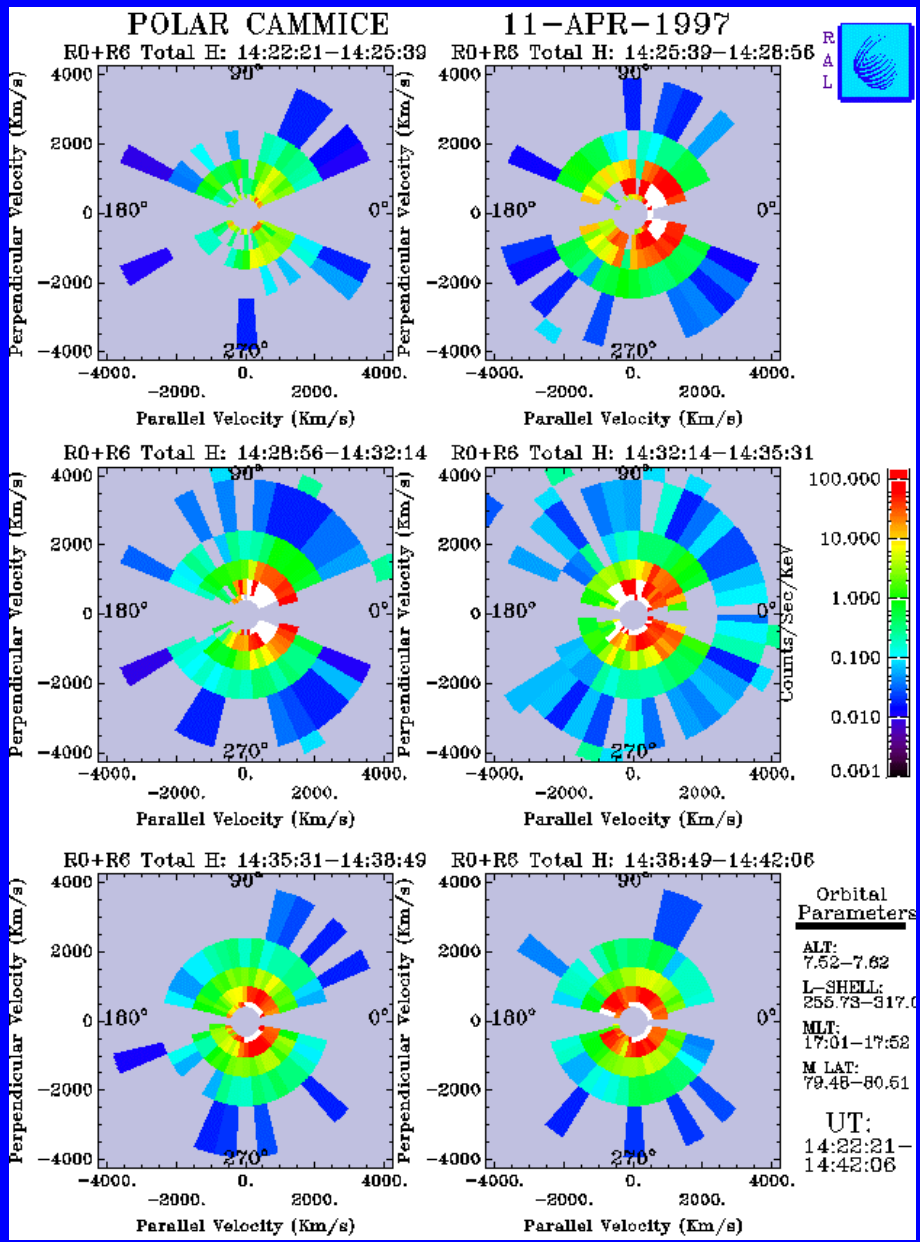

MG separatrix

+MP center, case A

MS ➪ electron separatrix

Event B:

Here Polar travels from the MS (PDL) to enter the reconnection outflow mostly on the MS side of the field reversal region, then back to MS. Note that on the MG side of B-field reversal region the hot ion skew is aligned.

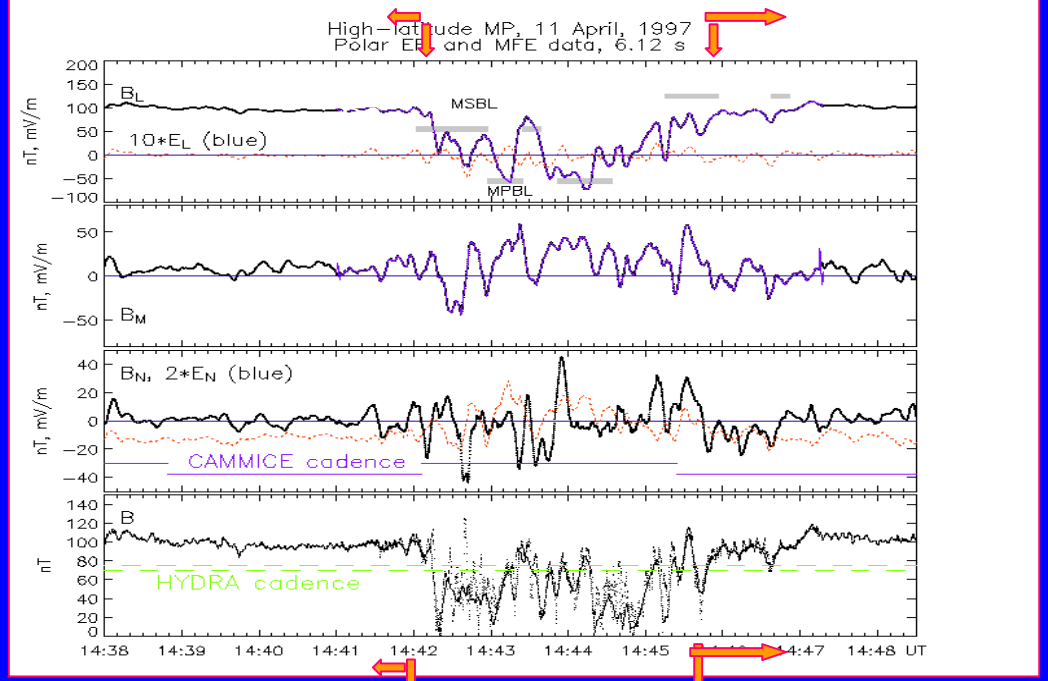

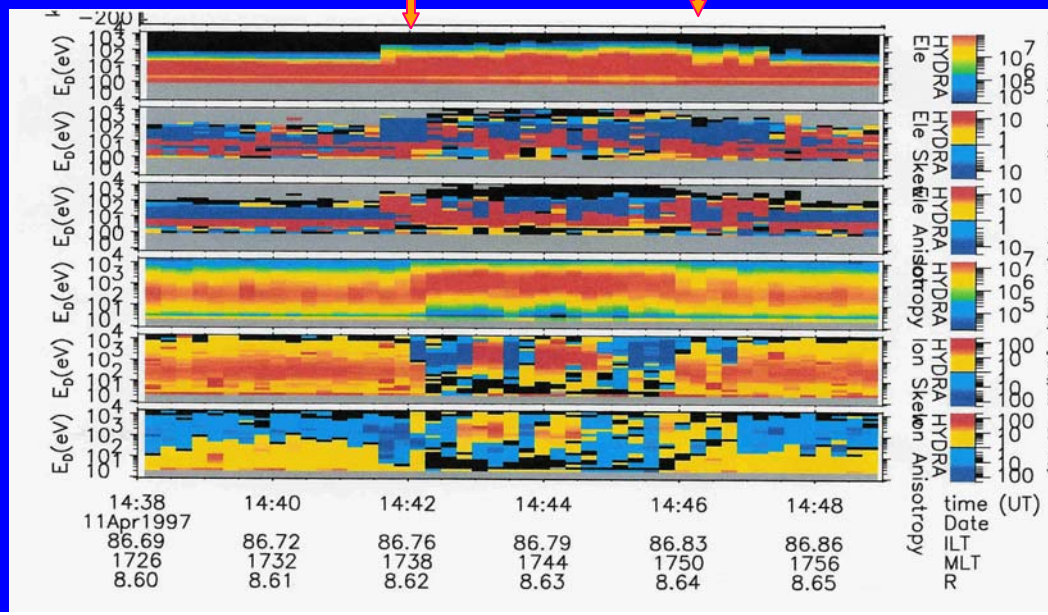

Arrows mark the region where Langmuir and/or upper hybrid waves were present

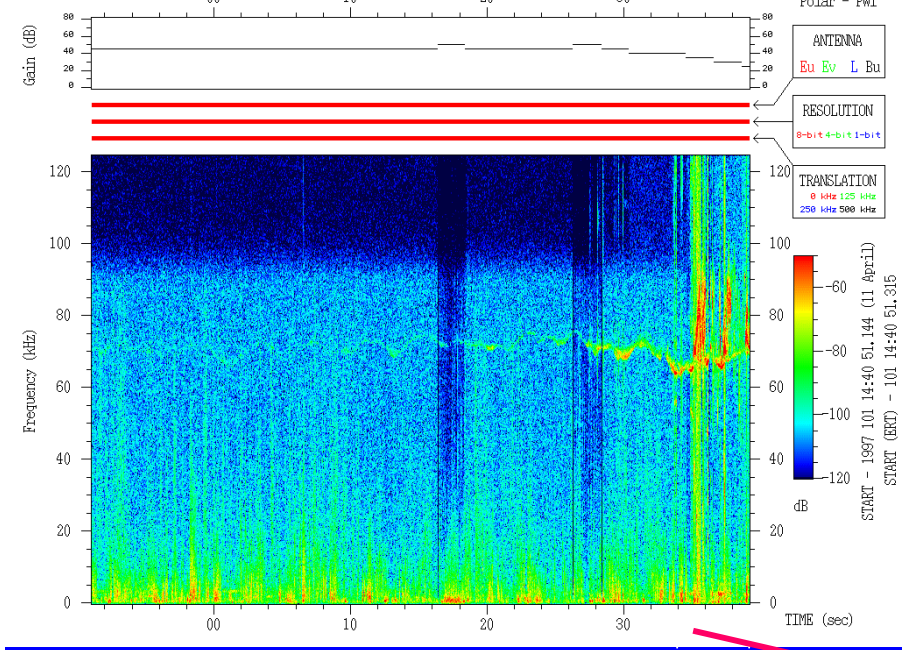

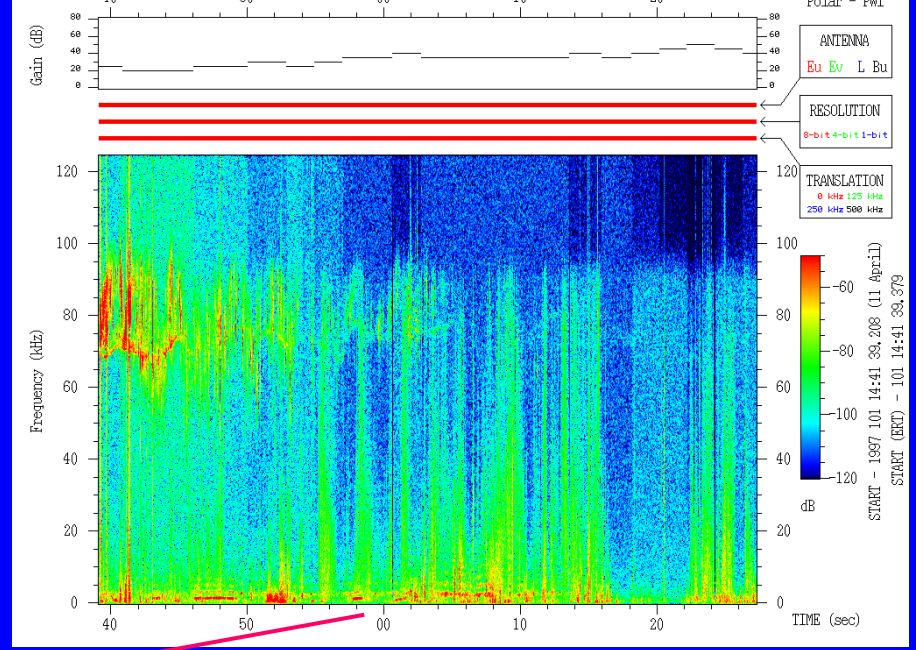

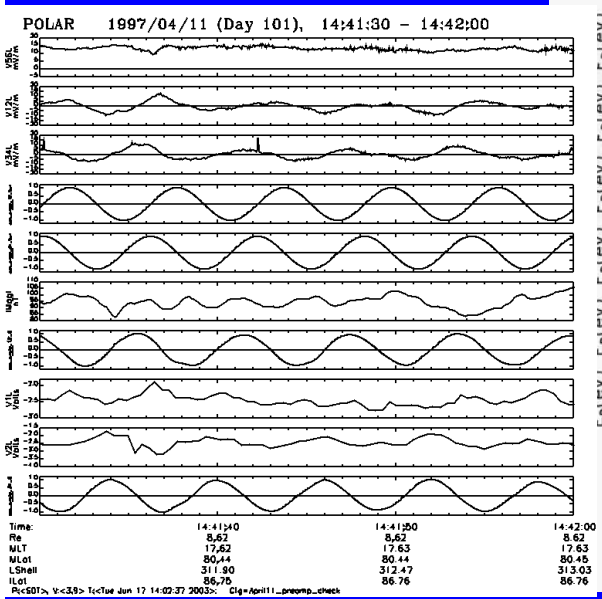

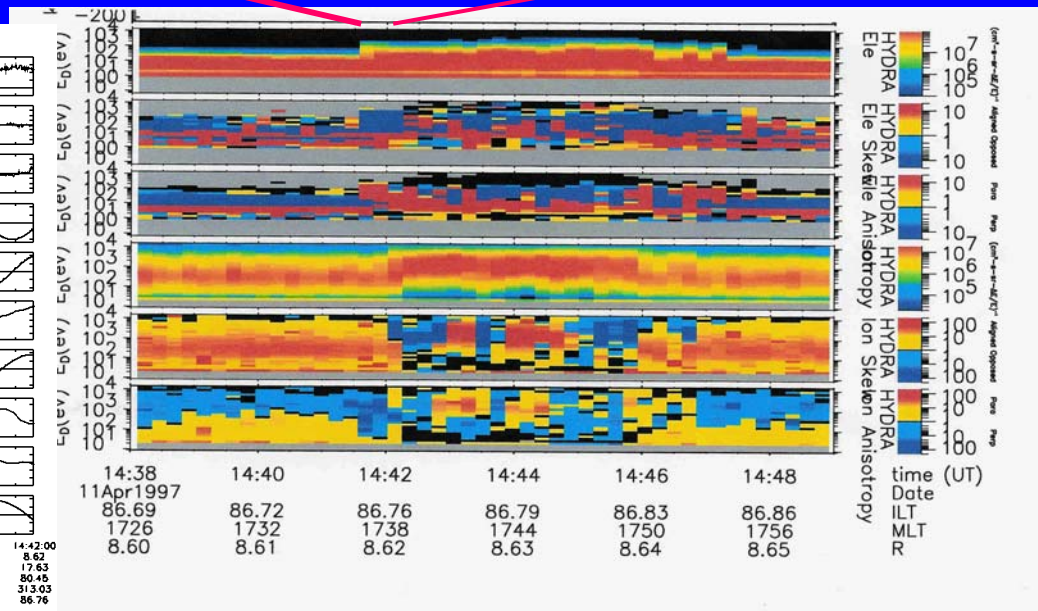

partial MP_i
event B1

Here Langmuir and up-/down-shifted electron acoustic (?) waves are seen within the electron separatrix on the MS side, 14:41:35-14:42:00 UT

Examples of waveforms confirming reality of Langmuir waves (but there are oth waves here, too):

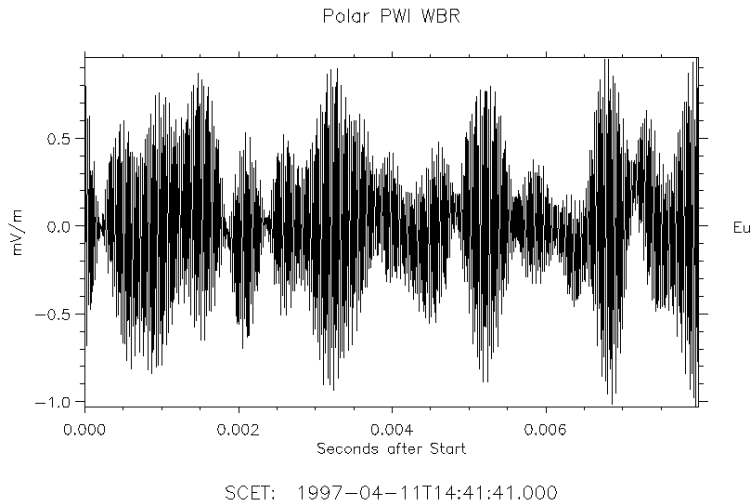

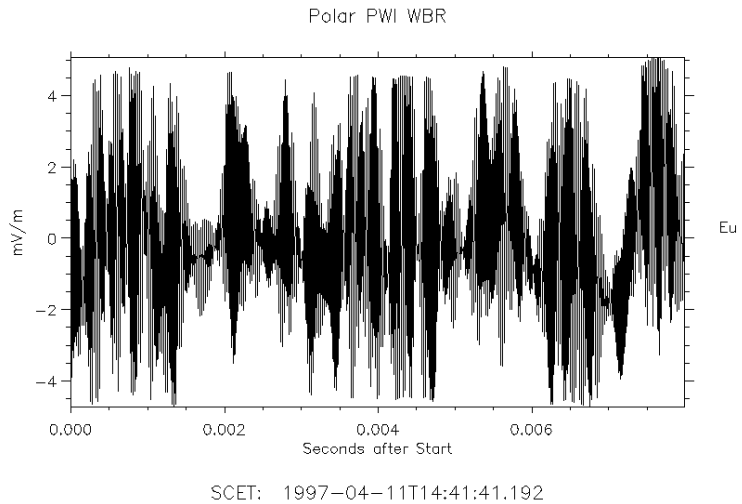

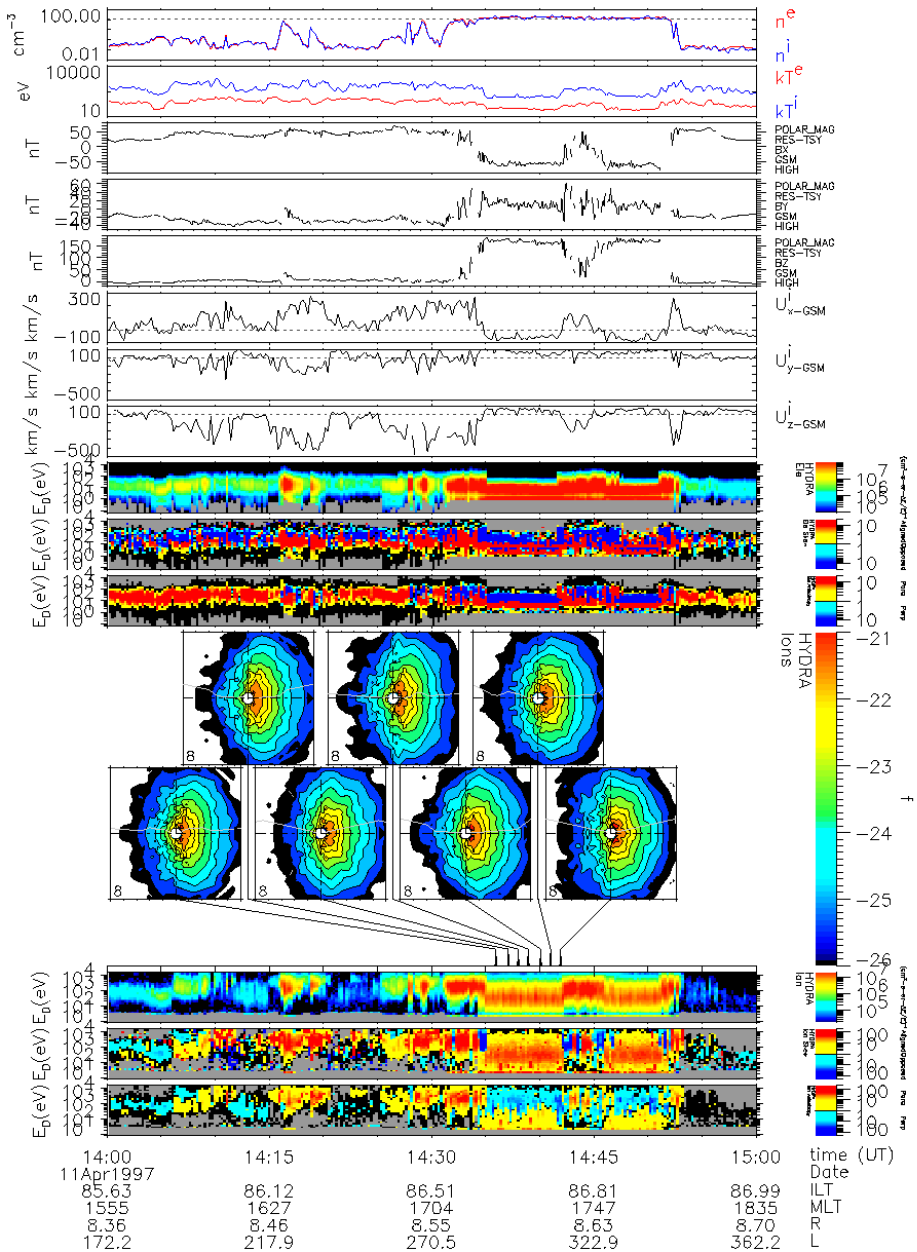
cm⁻³
100.00
0.01
n^e
n^i
eV
10000
10
kT^e
kT^i
nT
50
0
−50
POLAR_MAG
RES−TSY
BX
GSM
HIGH
nT
POLAR_MAG
RES−TSY
BY
GSM
HIGH
nT
150
100
50
0
POLAR_MAG
RES−TSY
BZ
GSM
HIGH
km/s
300
−100
U^i_x−GSM
km/s
100
−500
U^i_y−GSM
km/s
100
−500
U^i_z−GSM
E_D(eV)
HYDRA
Ions
−21
−22
−23
−24
−25
−26
14:00
11Apr1997
85.63
1555
8.36
172.2
14:15
86.12
1627
8.46
217.9
14:30
86.51
1704
8.55
270.5
14:45
86.81
1747
8.63
322.9
15:00
86.99
1835
8.70
362.2
time (UT)
Date
ILT
MLT
R
L

Electron holes (electron solitary waves) in the reconnection outflow region

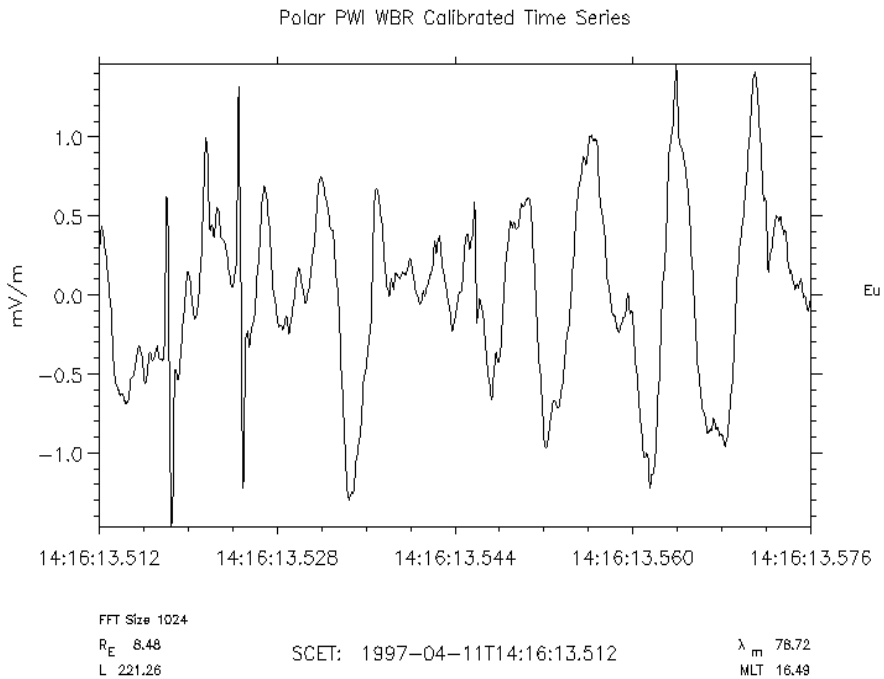

Fig. 10a

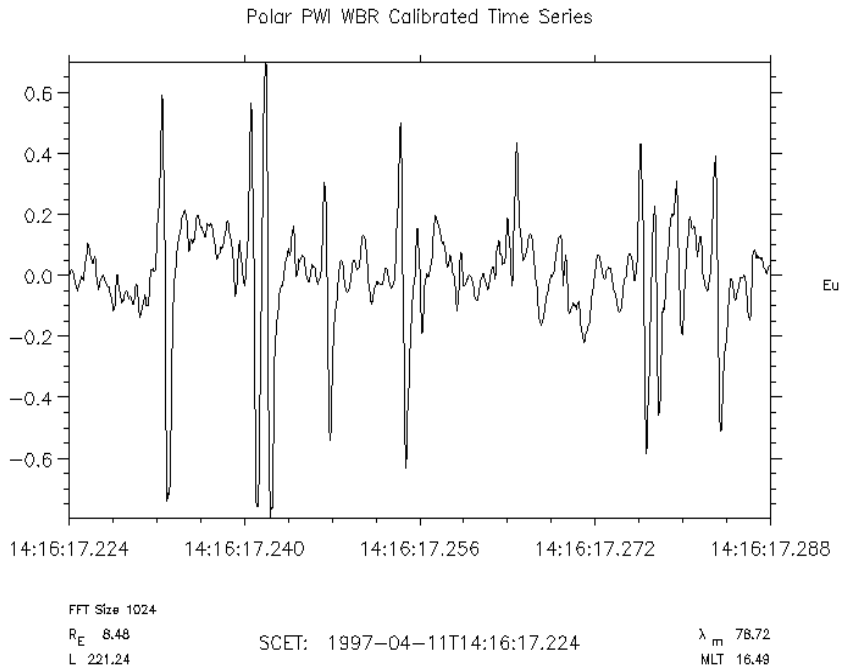

Fig. 10b

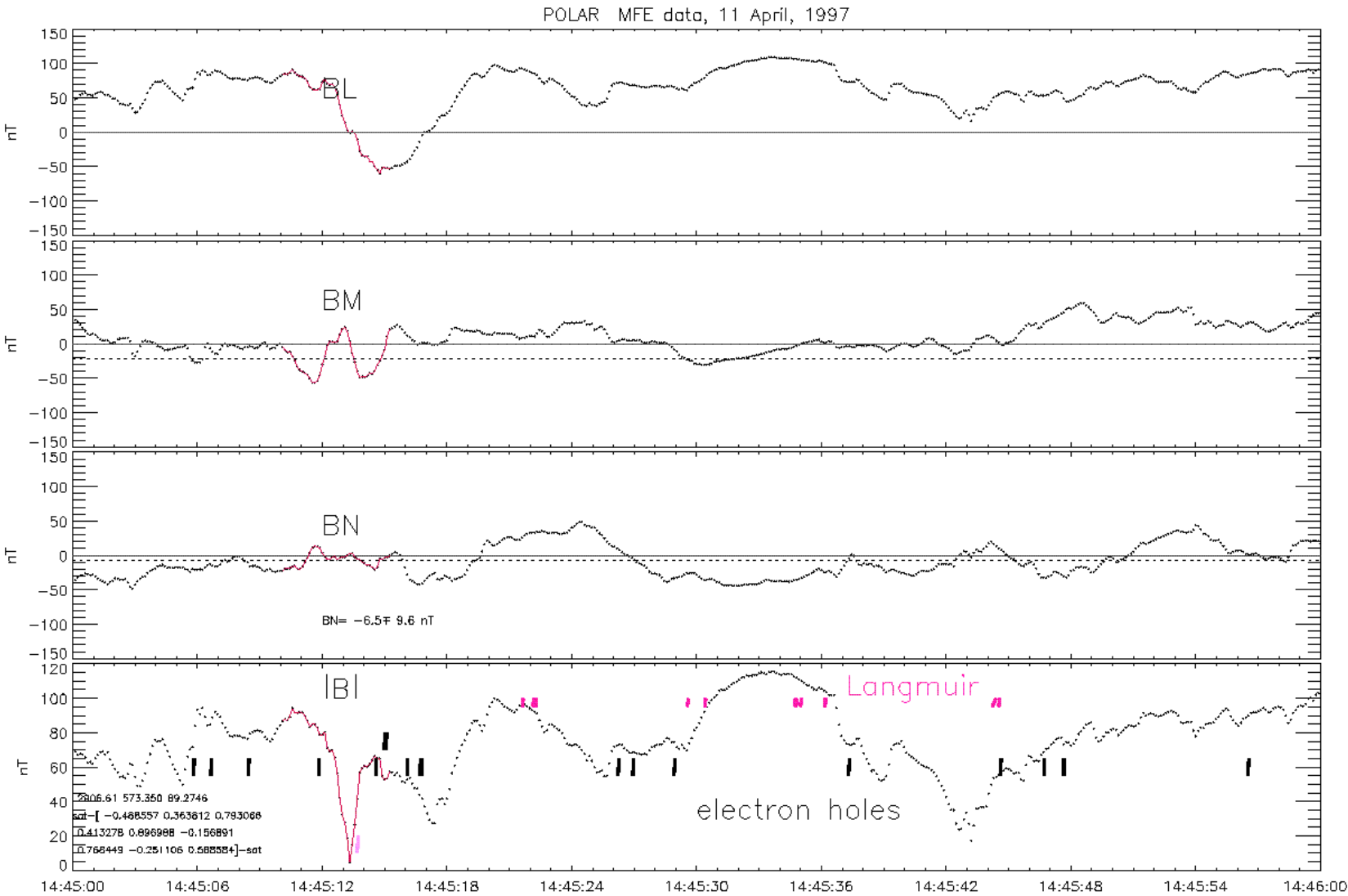
POLAR MFE data, 11 April, 1997
BL
BM
BN
BN= −6.5∓ 9.6 nT
|B|
Langmuir
electron holes
nT
14:45:00
14:45:06
14:45:12
14:45:18
14:45:24
14:45:30
14:45:36
14:45:42
14:45:48
14:45:54
14:46:00

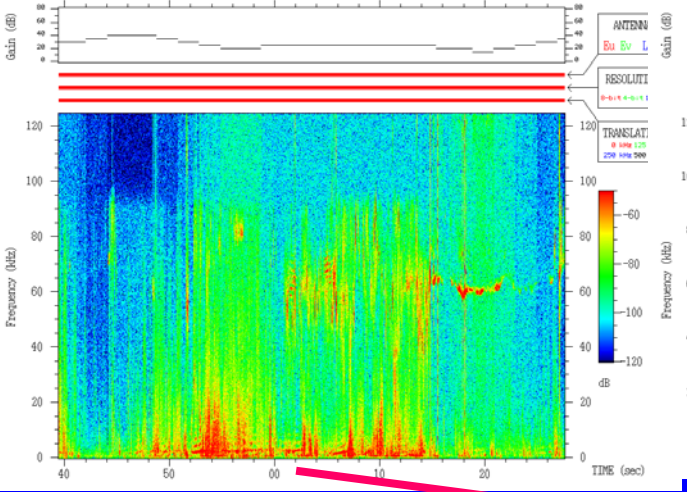

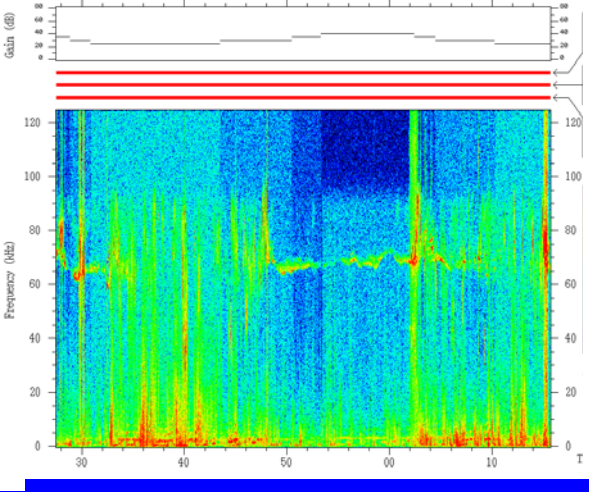

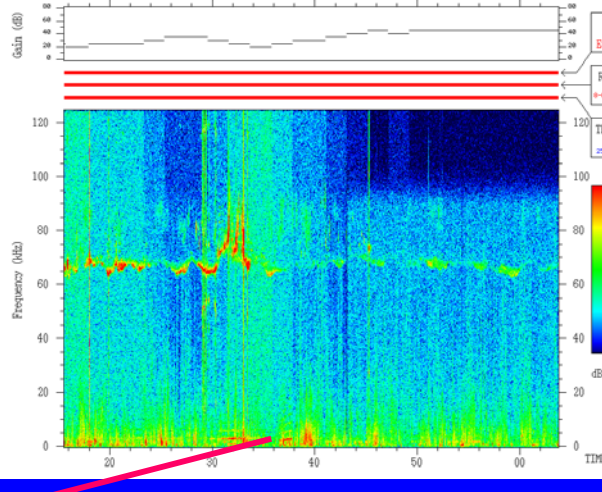

MSBL (mostly)
and MP_out, event B

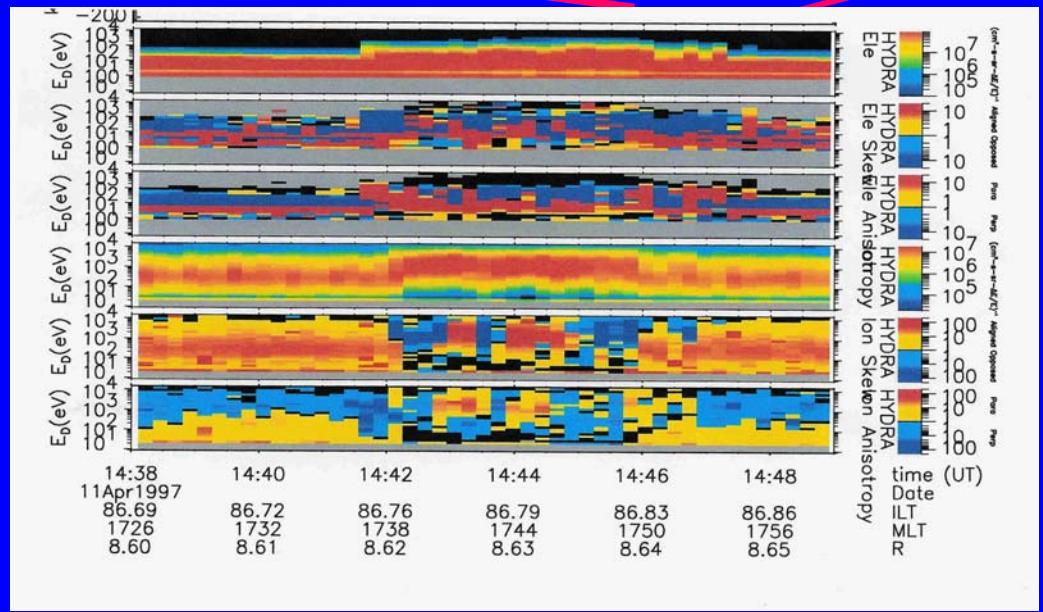

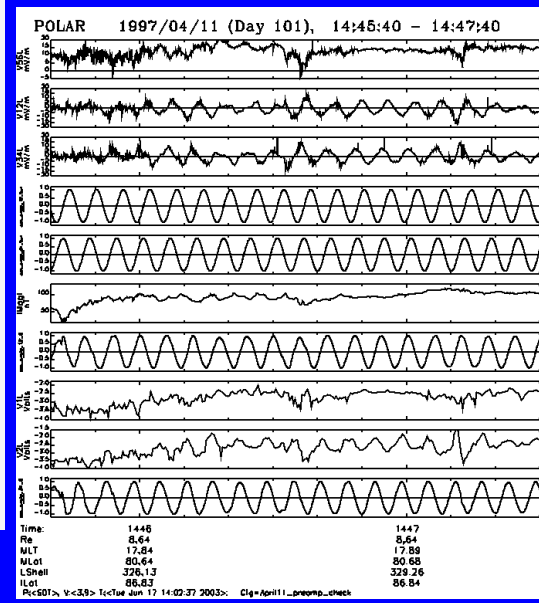

The same as on previous slide but for the next electron (and occasionally ion) separatrix on the MS side of the reconnection outflow, at 14:46:00-14:47:35. Note how the electron separatrix is well distinguished both on wave spectrograms and in the electric field data (smooth DC-field only).

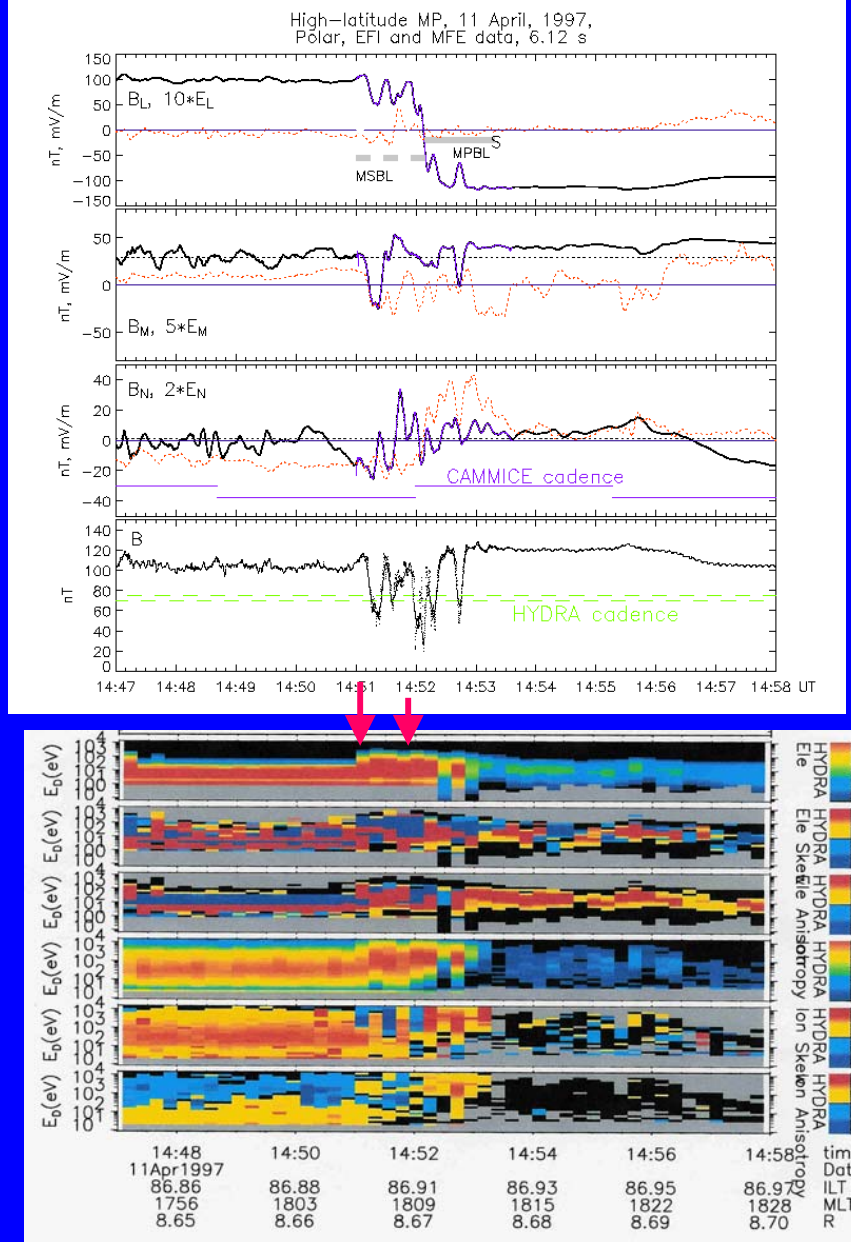

Event C

Arrows mark Langmuir waves occurrence during final MP_in

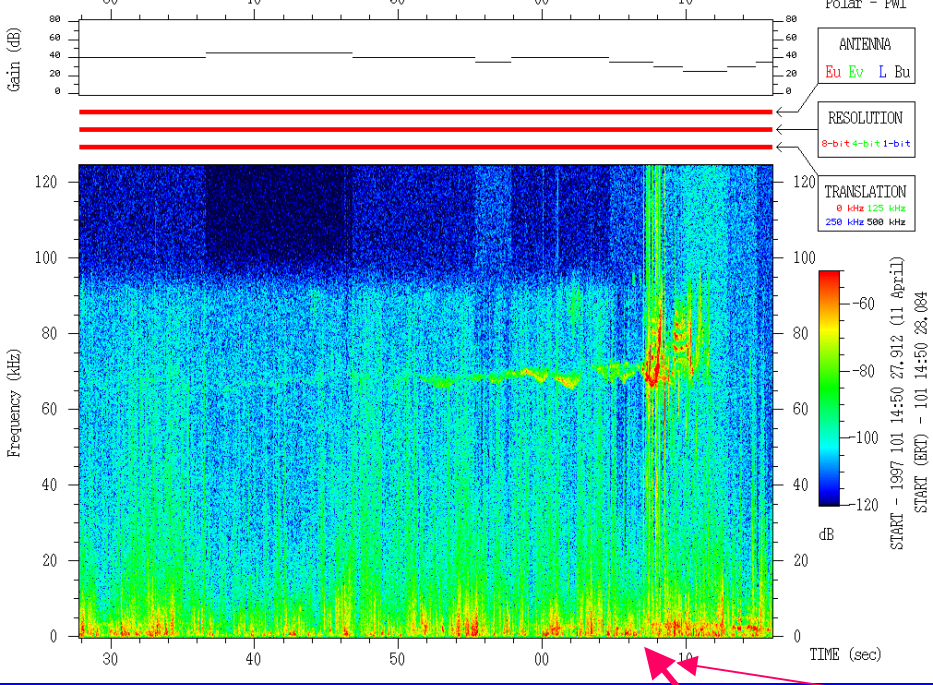

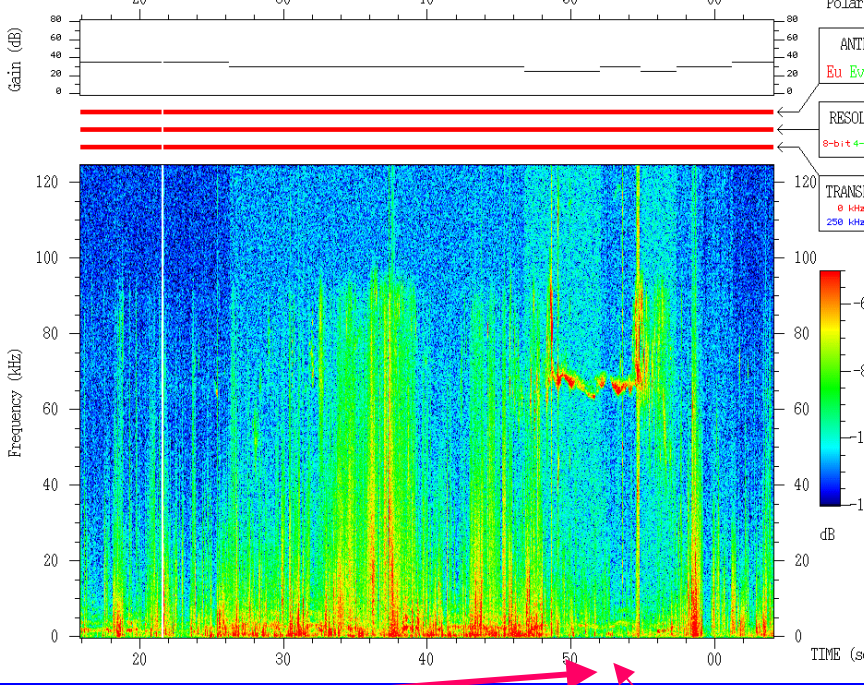

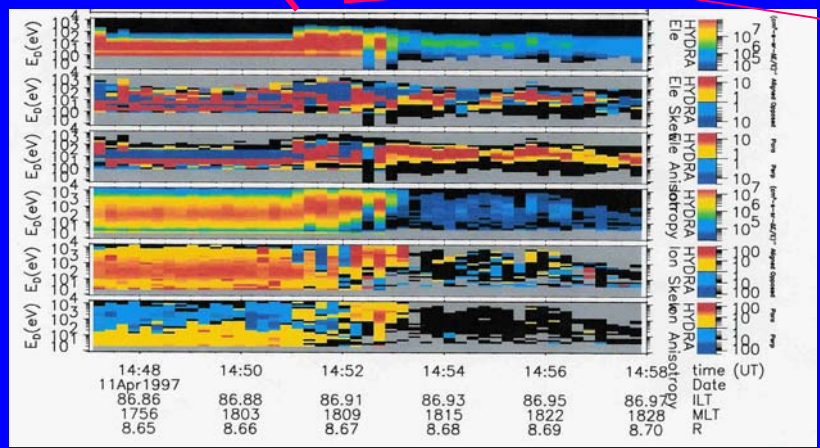

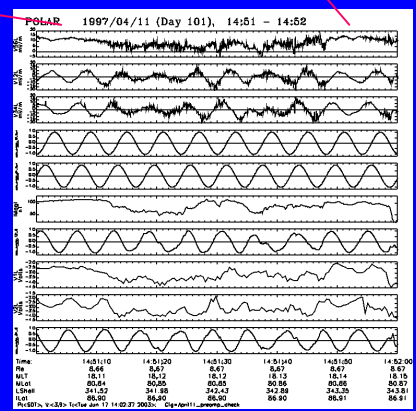

At 14:51:07-14:51:12 UT and 14:51:48-14:51:58 UT again at the separatrix on MS side during the final MP inbound crossing. (*Here only Hydra 3-s spectra can help to resolve the structure, i.e., electron vs ion separatrix. Smooth DC electric field indicates electron separatrix ?*)

MS, PDL

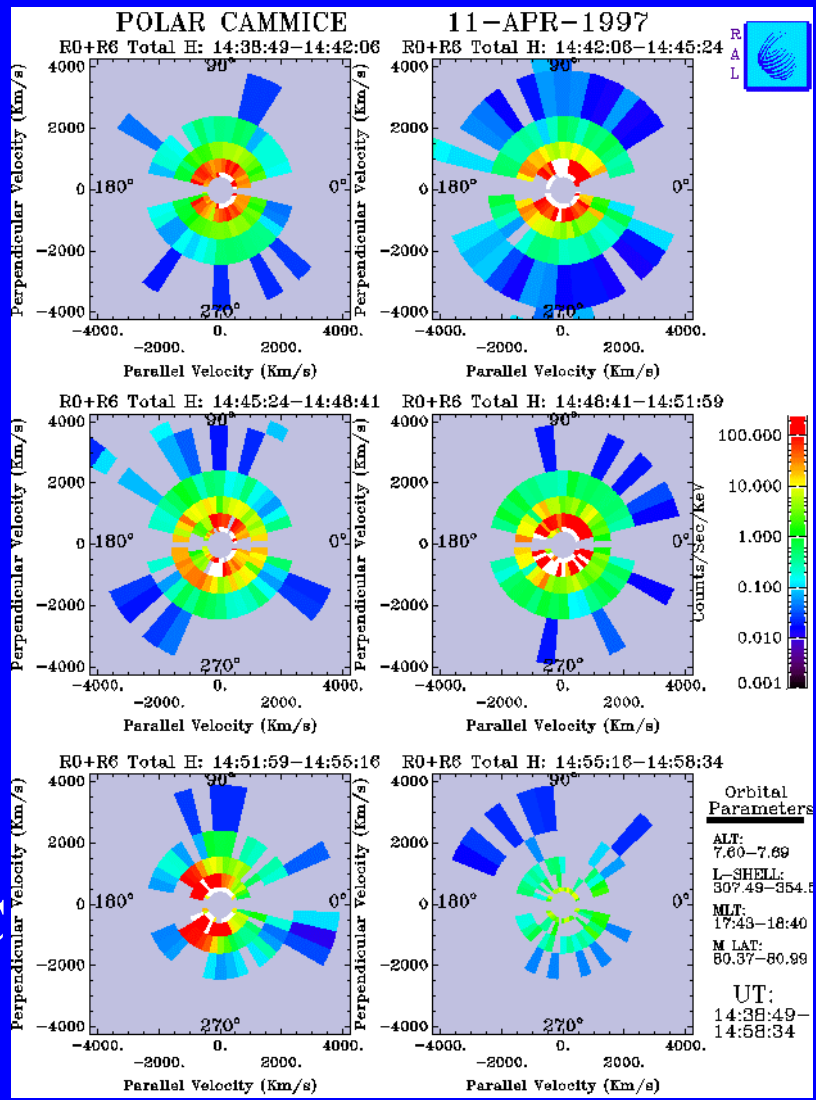

MP_in, case C

lobe

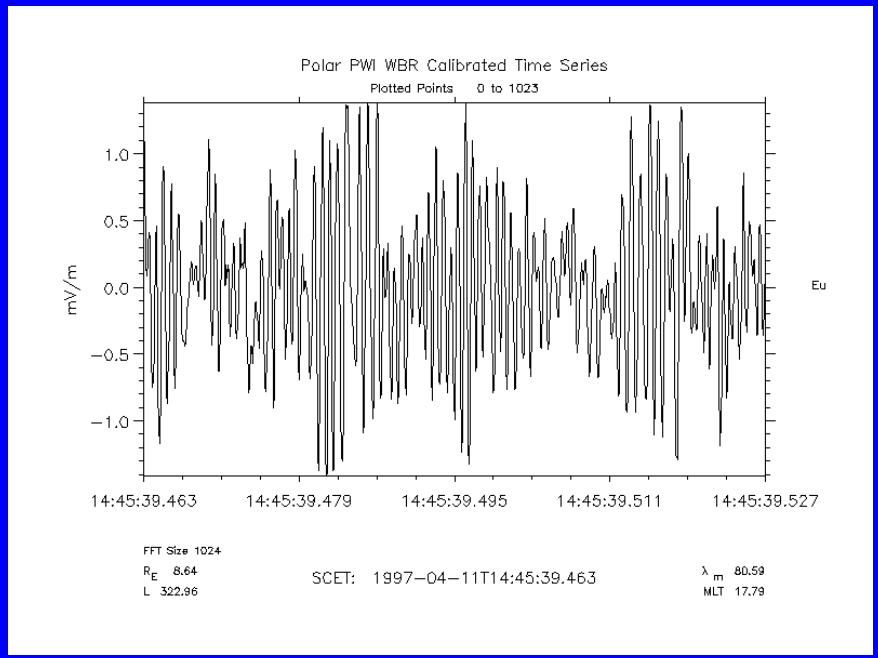

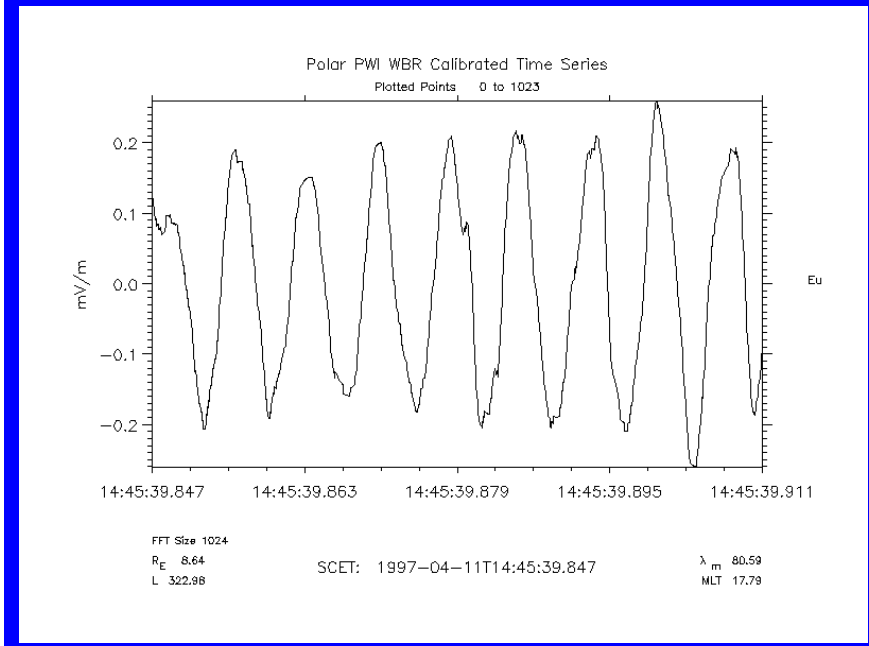

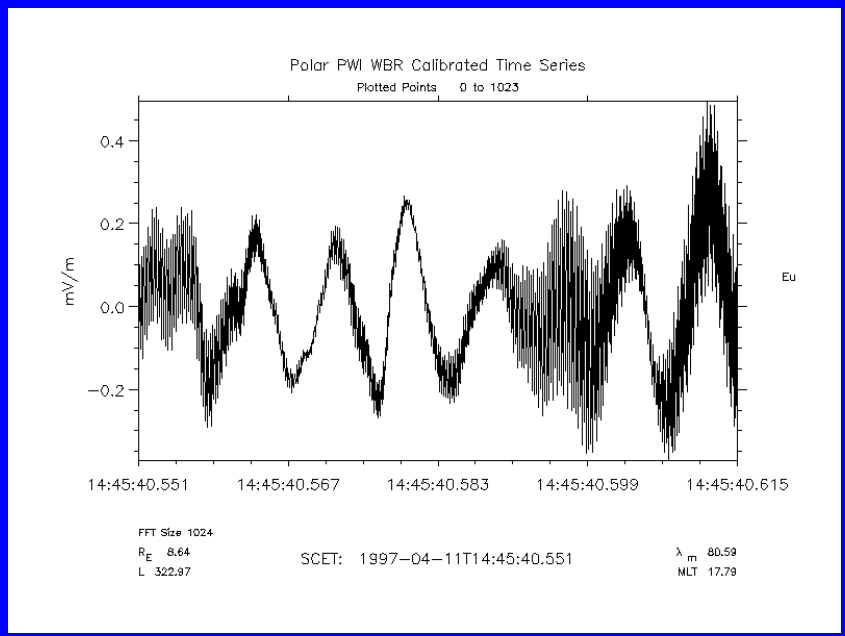

Kąt anteny względem B:
93^{o} -137^{o}

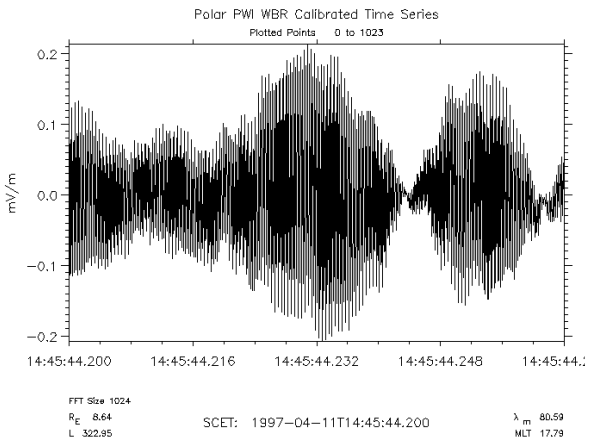
Polar PWI WBR Calibrated Time Series
Plotted Points 0 to 1023
mV/m
0.2
0.1
0.0
−0.1
−0.2
14:45:44.200
14:45:44.216
14:45:44.232
14:45:44.248
FFT Size 1024
R_E 8.64
L 322.95
SCET: 1997−04−11T14:45:44.200
λ_m 80.59
MLT 17.79

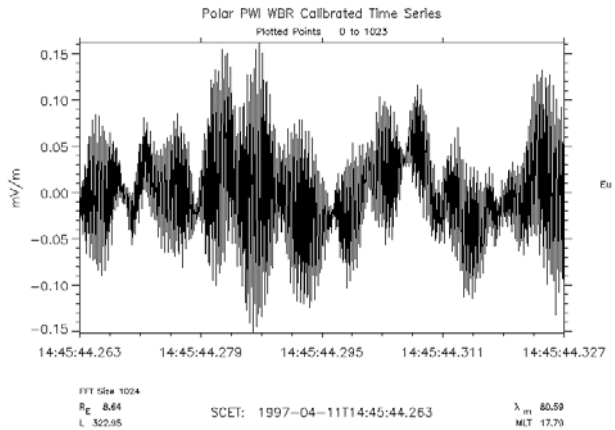
Polar PWI WBR Calibrated Time Series
Plotted Points 0 to 1023
mV/m
0.15
0.10
0.05
0.00
−0.05
−0.10
−0.15
14:45:44.263
14:45:44.279
14:45:44.295
14:45:44.311
14:45:44.327
FFT Size 1024
R_E 8.64
L 322.95
SCET: 1997−04−11T14:45:44.263
λ_m 80.59
MLT 17.79

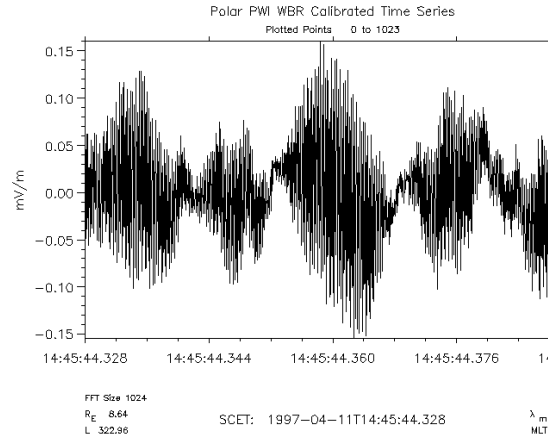
Polar PWI WBR Calibrated Time Series
Plotted Points 0 to 1023
mV/m
0.15
0.10
0.05
0.00
−0.05
−0.10
−0.15
14:45:44.328
14:45:44.344
14:45:44.360
14:45:44.376
FFT Size 1024
R_E 8.64
L 322.96
SCET: 1997−04−11T14:45:44.328

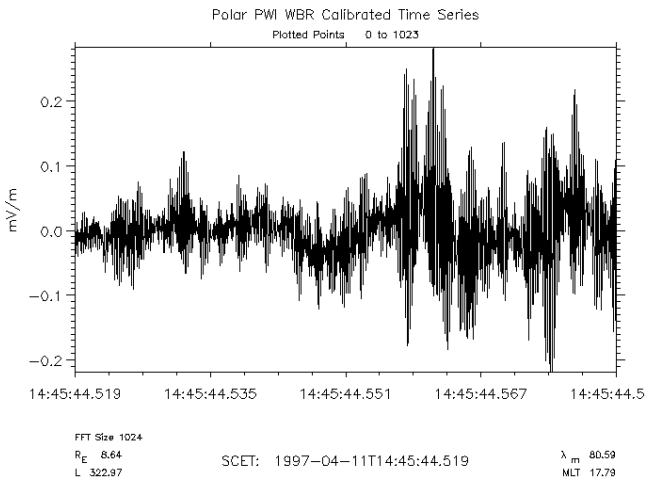
Polar PWI WBR Calibrated Time Series
Plotted Points 0 to 1023
mV/m
0.2
0.1
0.0
−0.1
−0.2
14:45:44.519
14:45:44.535
14:45:44.551
14:45:44.567
FFT Size 1024
R_E 8.64
L 322.97
SCET: 1997−04−11T14:45:44.519
λ_m 80.59
MLT 17.79

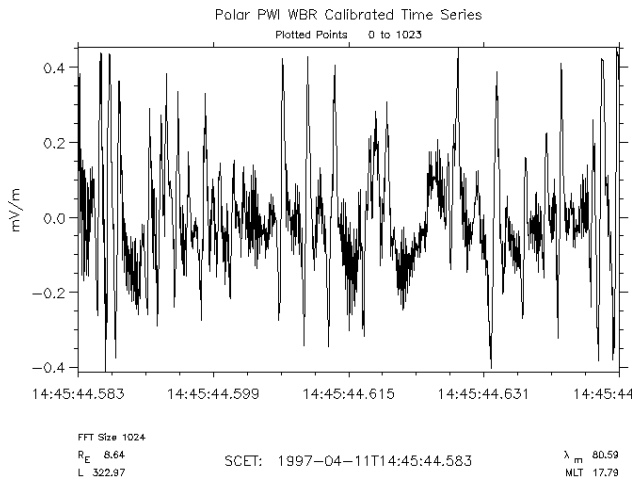
Polar PWI WBR Calibrated Time Series
Plotted Points 0 to 1023
mV/m
0.4
0.2
0.0
−0.2
−0.4
14:45:44.583
14:45:44.599
14:45:44.615
14:45:44.631
FFT Size 1024
R_E 8.64
L 322.97
SCET: 1997−04−11T14:45:44.583
λ_m 80.59
MLT 17.79

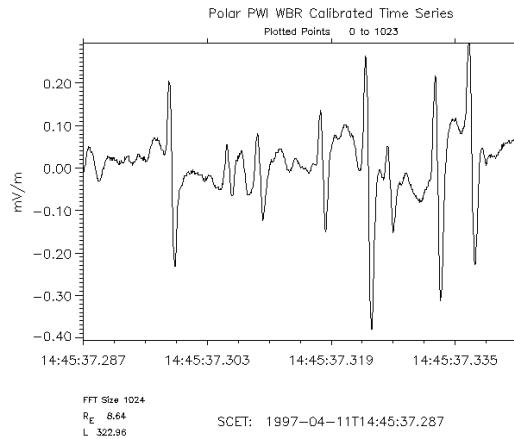
Polar PWI WBR Calibrated Time Series
Plotted Points 0 to 1023
mV/m
0.20
0.10
0.00
−0.10
−0.20
−0.30
−0.40
14:45:37.287
14:45:37.303
14:45:37.319
14:45:37.335
FFT Size 1024
R_E 8.64
L 322.96
SCET: 1997−04−11T14:45:37.287

SUMMARY

We try to find a coherent scenario that produce turbulent boundary layer at the high-latitude magnetopause under strong northward IMF. Low temporal resolution of plasma data make it difficult. Merging site seems to be structured on much finer scales.

Wave data from Wide Band Receiver (WBR) are very helpful i studies on physical process responsible for such a structuring.

EFI data: A compression of the magnetic field was found at the magnetospheric separatrix , co-existent with a sharp minimum of local plasma density, as predicted by, *Shay et al., 2001* simulation of magneti reconnection using electron PIC code. Intense lower hybrid turbulence i seen at the density gradient within the separatrix on the magnetospheric side of the outflow region.

Electromagnetic wave packets of whistlers type as well as electron holes are found at the walls of magnetic cavities. Electron holes were predicted to form in the reconnection outflow region by recent simulations of *Drake et al., 2003* (*Science, Vol. 299*) and are signs of electron-scale physics domination in the merging site.

PWI data: We found that Langmuir and/or upper hybrid waves occur as dominant waves in the narrow region of electron separatrix bordering the sunward outflow region on the magnetosheath side of the current layer. These waves may be excited by ``bump on the tail'' instability.

Slightly deeper into the outflow region where hot ion beams appear and hot electron beam is denser, Langmuir waves may coalesce into electron solitary waves.

SUMMARY –cont.

On the magnetospheric side of the outflow region we may have bi-stream instability (counterstreaming equally dense hot electron beams and hot ion beam) and it is probably why electron holes are so abundant there (e. g., *Omura et al., 1996*).

Coupling of electron solitary and Langmuir/upper hybrid wave to lower hybrid waves in different regions of merging site - next subject to study.

.

Earlier observations of Langmuir waves at the magnetopause: - Gurnett et al., 1979

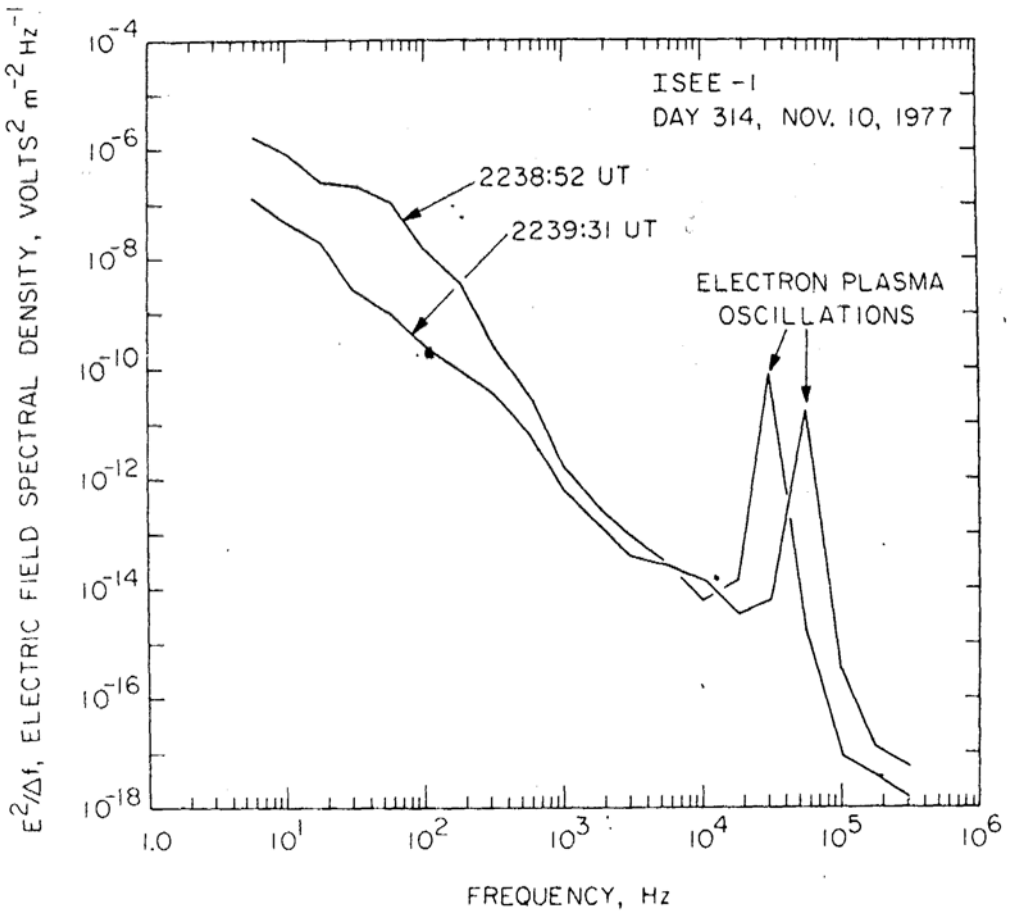

Fig. 13. Selected electric field spectra from the magnetopause crossing in Figures 4 and 5 showing the occurrence of intense narrow-band emissions near the local electron plasma frequency.

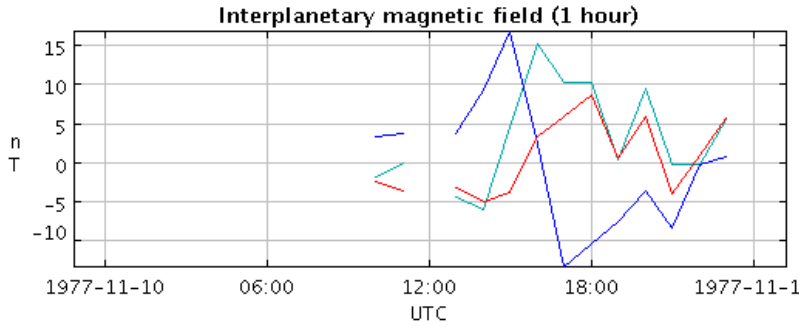

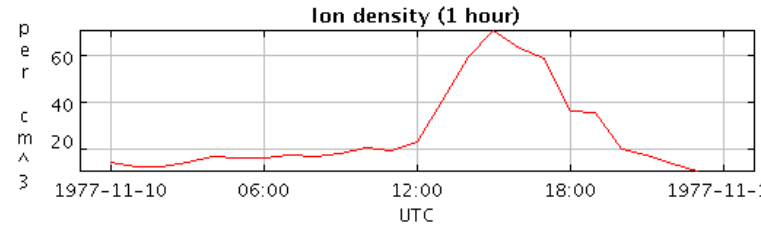

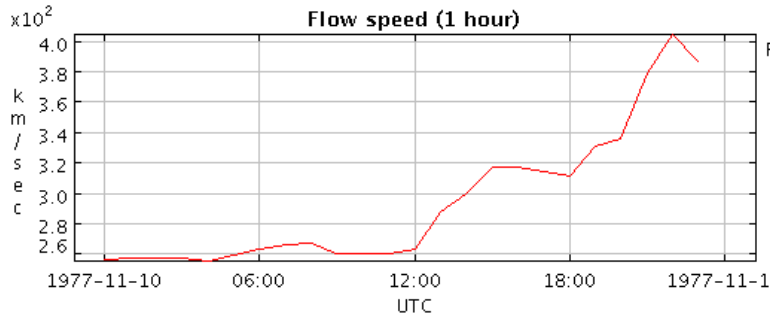

Striking similarity of high-frequency waves in the foreshock and at this magnetopause:

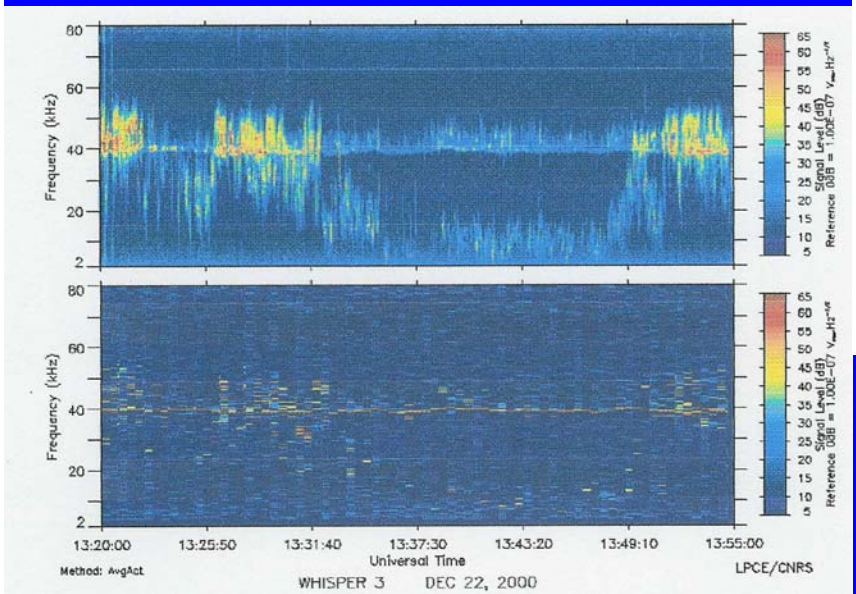

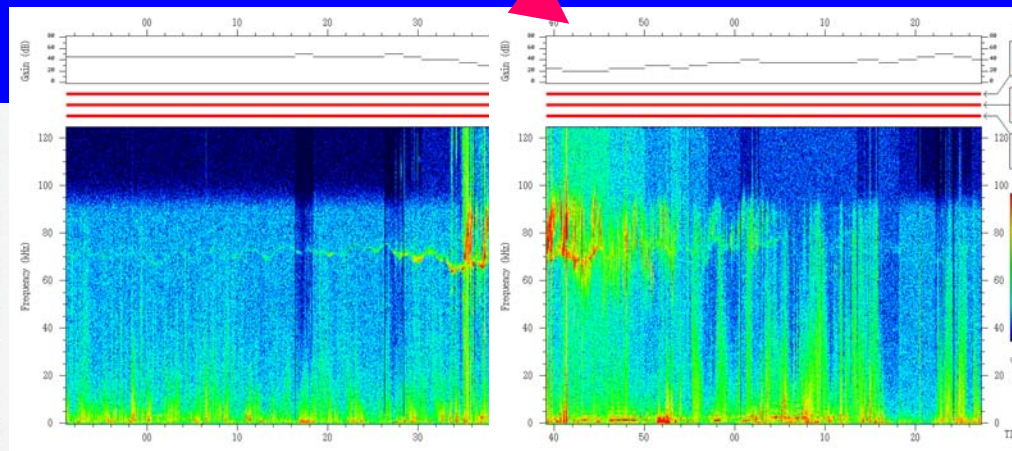

*Left:*Cluster, Samba, Whisper data - waves in the foreshock region of the bow shock, from Décréau et al., 2001, their Fig. 10. *Upper panel* - Natural wave mode, *lower panel*- Sounding wave mode. *Right*: Polar, PWI, WBR spectra, MS, electron separatrix and the reconnection outflow region at the high-latitude magnetopause.

Acknowledgments*: *This work was done in the frame of European Research Training Network "Turbulent Boundary Layers in Geospace Plasmas" under contract HPRN-CT-2001-00314.

END

Why V1L
is so “dull”?

Event A

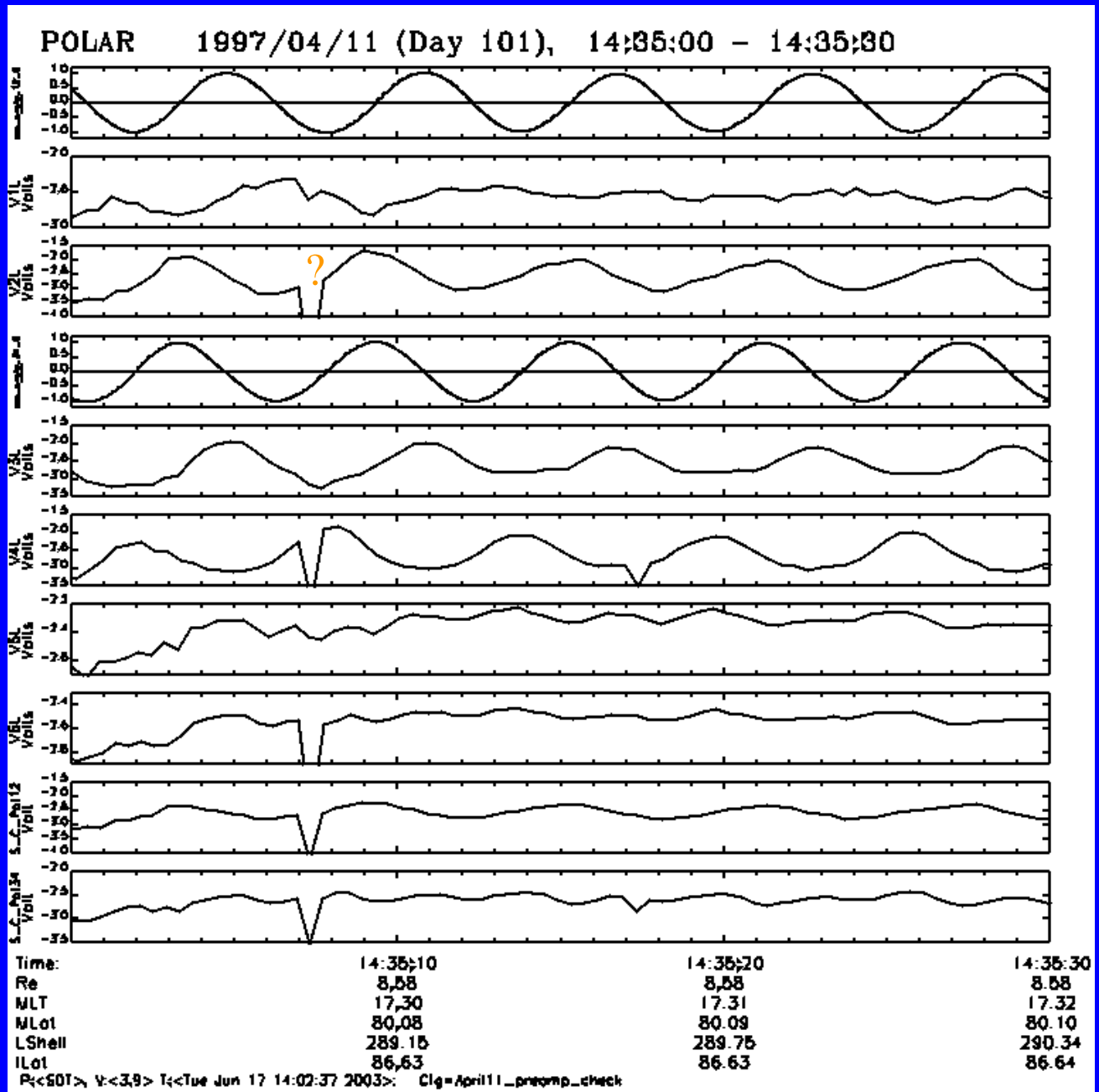

Event B1

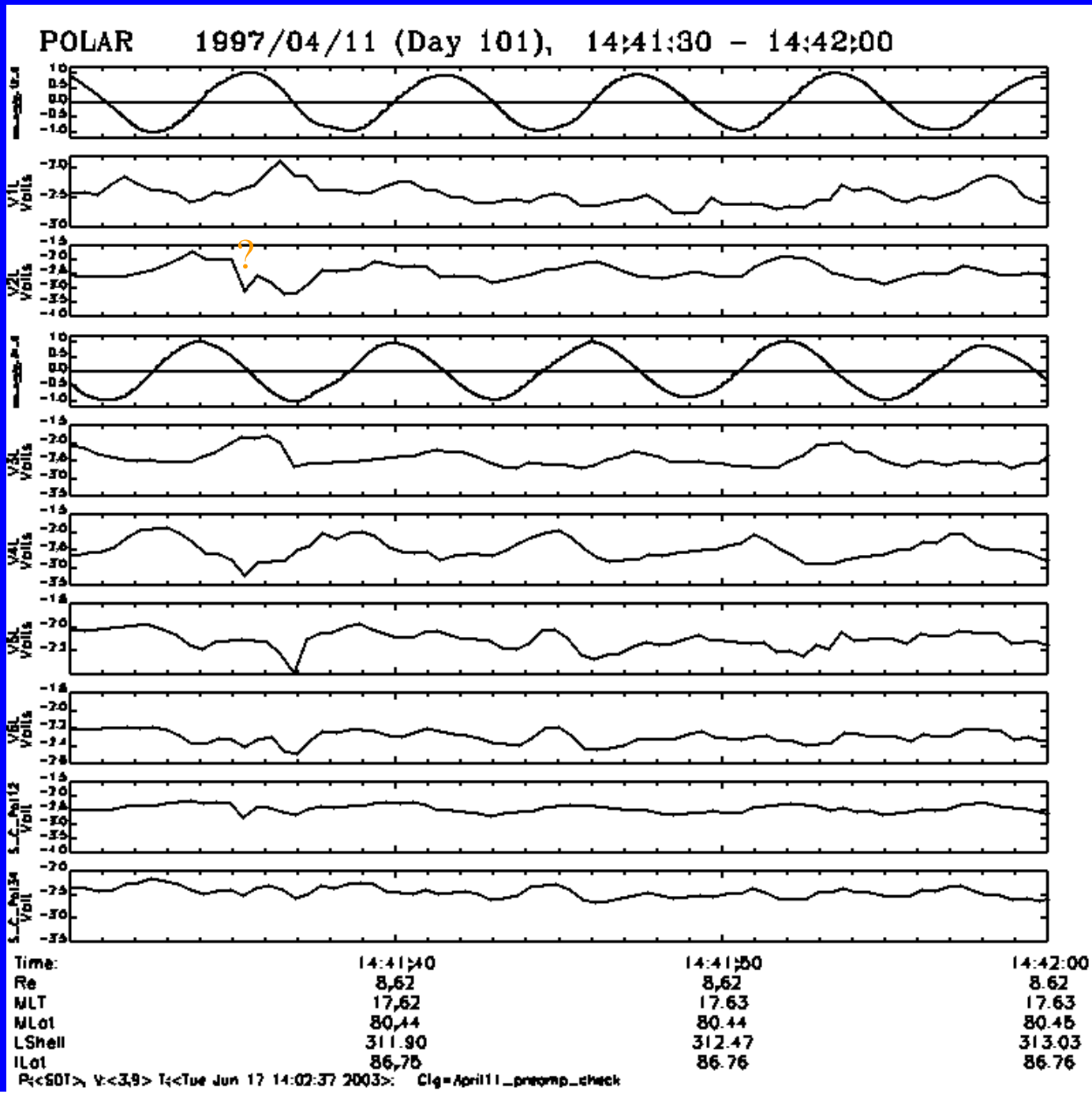
POLAR 1997/04/11 (Day 101), 14:41:30 - 14:42:00
V1L Volts
V2L Volts
V3L Volts
V4L Volts
V5L Volts
V6L Volts
S_C_Pol12 Volt
S_C_Pol34 Volt
?
Time: 14:41:40 14:41:50 14:42:00
Re 8.62 8.62 8.62
MLT 17.62 17.63 17.63
MLat 80.44 80.44 80.45
LShell 311.90 312.47 313.03
ILat 86.75 86.76 86.76
P:<SOT>, V:<3.9> T:<Tue Jun 17 14:02:37 2003>: Cfg=April11_preamp_check

Event B2

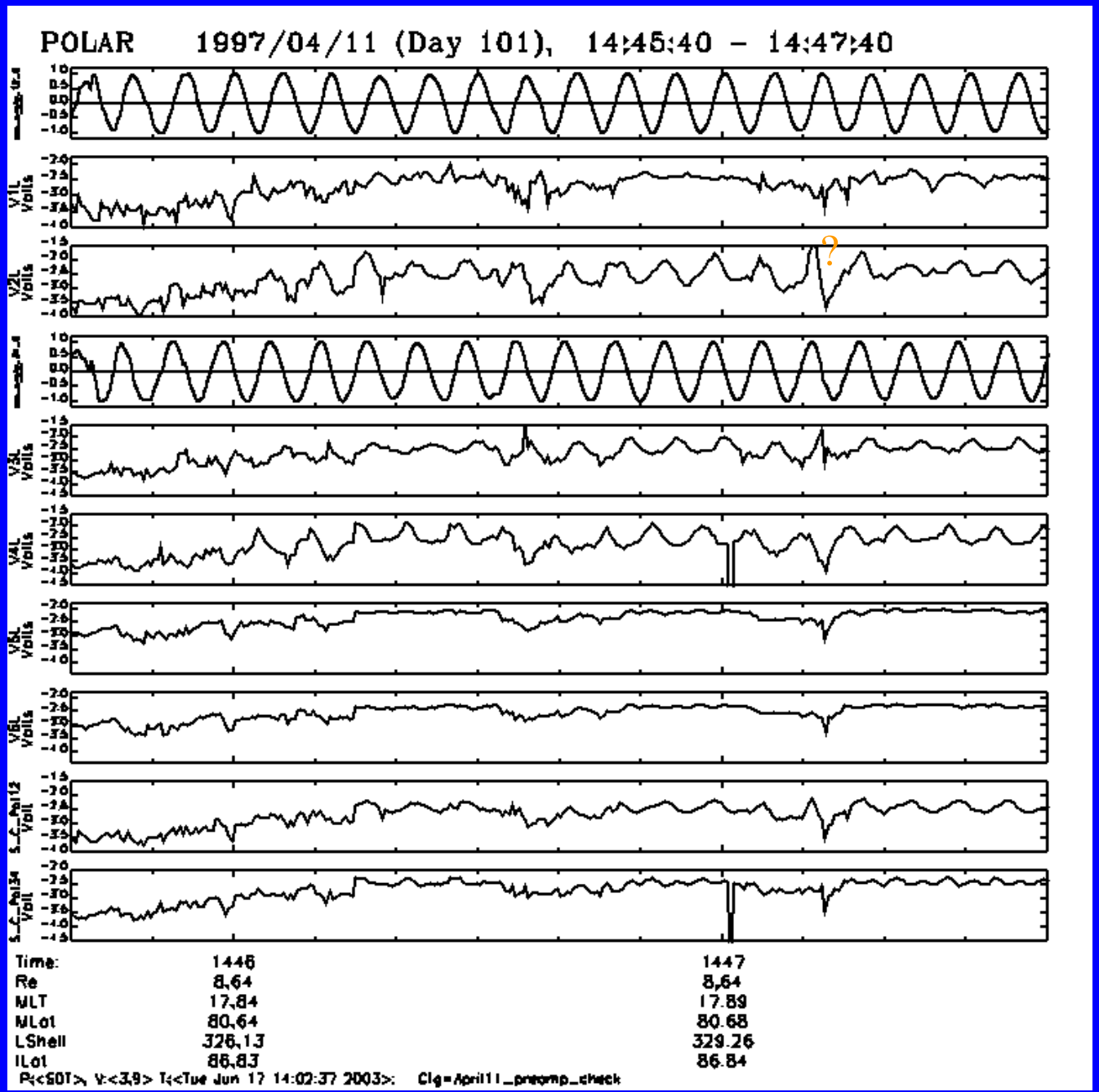
POLAR 1997/04/11 (Day 101), 14:45:40 - 14:47:40
V1L Volts
V2L Volts
V3L Volts
V4L Volts
V5L Volts
V6L Volts
S_C_Pol12 Volt
S_C_Pol34 Volt
?
Time: 1446 1447
Re 8.64 8.64
MLT 17.84 17.89
MLat 80.64 80.68
LShell 326.13 329.26
ILat 86.83 86.84
P:<SOT> V:<3.9> T:<Tue Jun 17 14:02:37 2003>: Cfg=April11_preamp_check

Event C

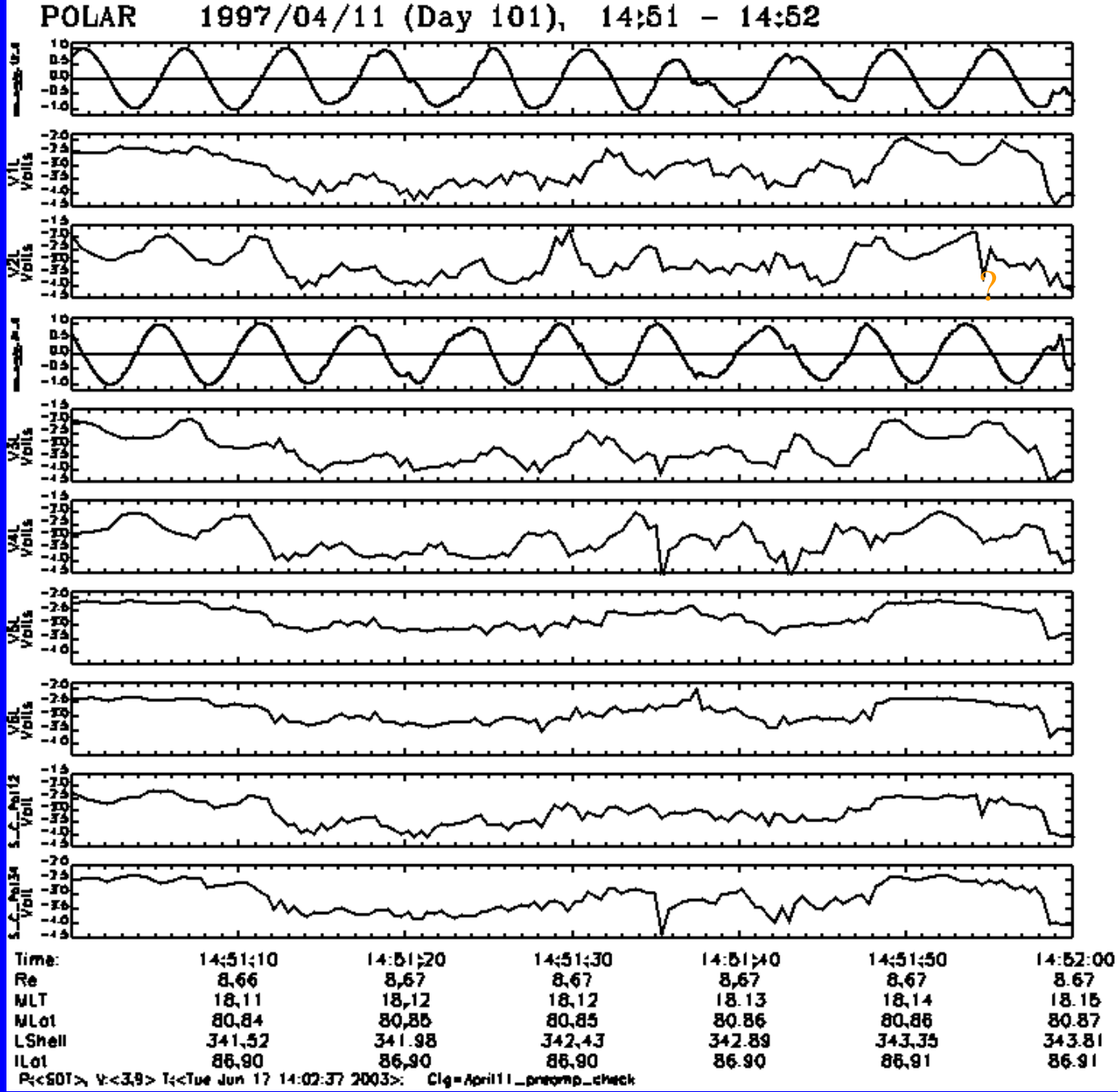
POLAR 1997/04/11 (Day 101), 14:51 - 14:52
V1L Volts
V2L Volts
?
V3L Volts
V4L Volts
V5L Volts
V6L Volts
S_C_Pot12 Volt
S_C_Pot34 Volt
Time: 14:51:10 14:51:20 14:51:30 14:51:40 14:51:50 14:52:00
Re 8.66 8.67 8.67 8.67 8.67 8.67
MLT 18.11 18.12 18.12 18.13 18.14 18.15
MLat 80.84 80.85 80.85 80.86 80.86 80.87
LShell 341.52 341.98 342.43 342.89 343.35 343.81
ILat 86.90 86.90 86.90 86.90 86.91 86.91
P:<SOT> V:<3.9> T:<Tue Jun 17 14:02:37 2003>: Cfg=April11_preamp_check

Higher resolution EFI data (V12,V34,V56) during the same four intervals:

Event A

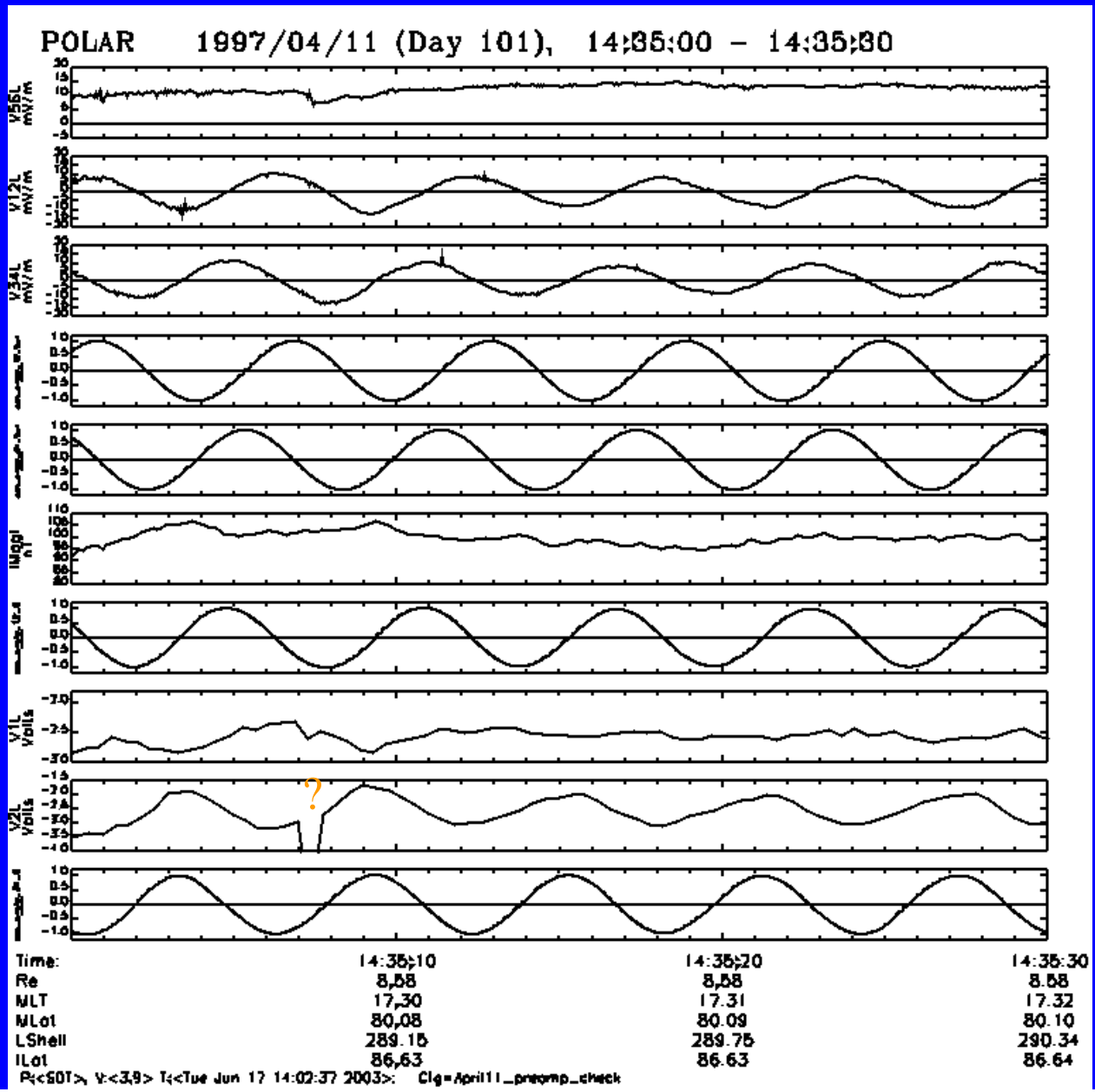

Event B1

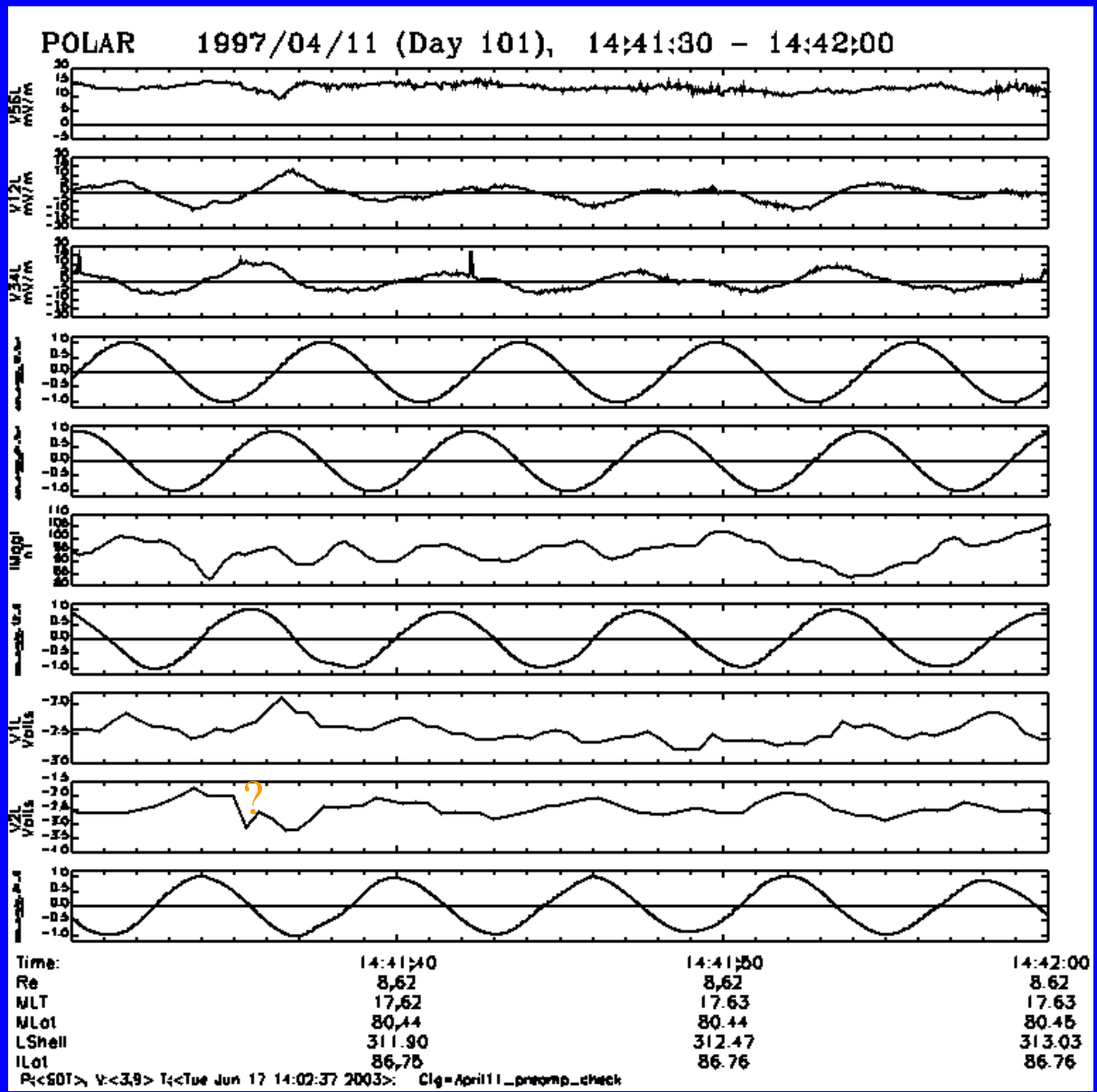
POLAR 1997/04/11 (Day 101), 14:41:30 - 14:42:00
V56L mV/m
V12L mV/m
V34L mV/m
Wgpl nT
V1L Volts
V2L Volts
?
Time: 14:41:40 14:41:50 14:42:00
Re 8.62 8.62 8.62
MLT 17.62 17.63 17.63
MLat 80.44 80.44 80.45
LShell 311.90 312.47 313.03
ILat 86.75 86.76 86.76
P:<SOT>, V:<3.9> T:<Tue Jun 17 14:02:37 2003>: Cfg=April11_preamp_check

Event B2

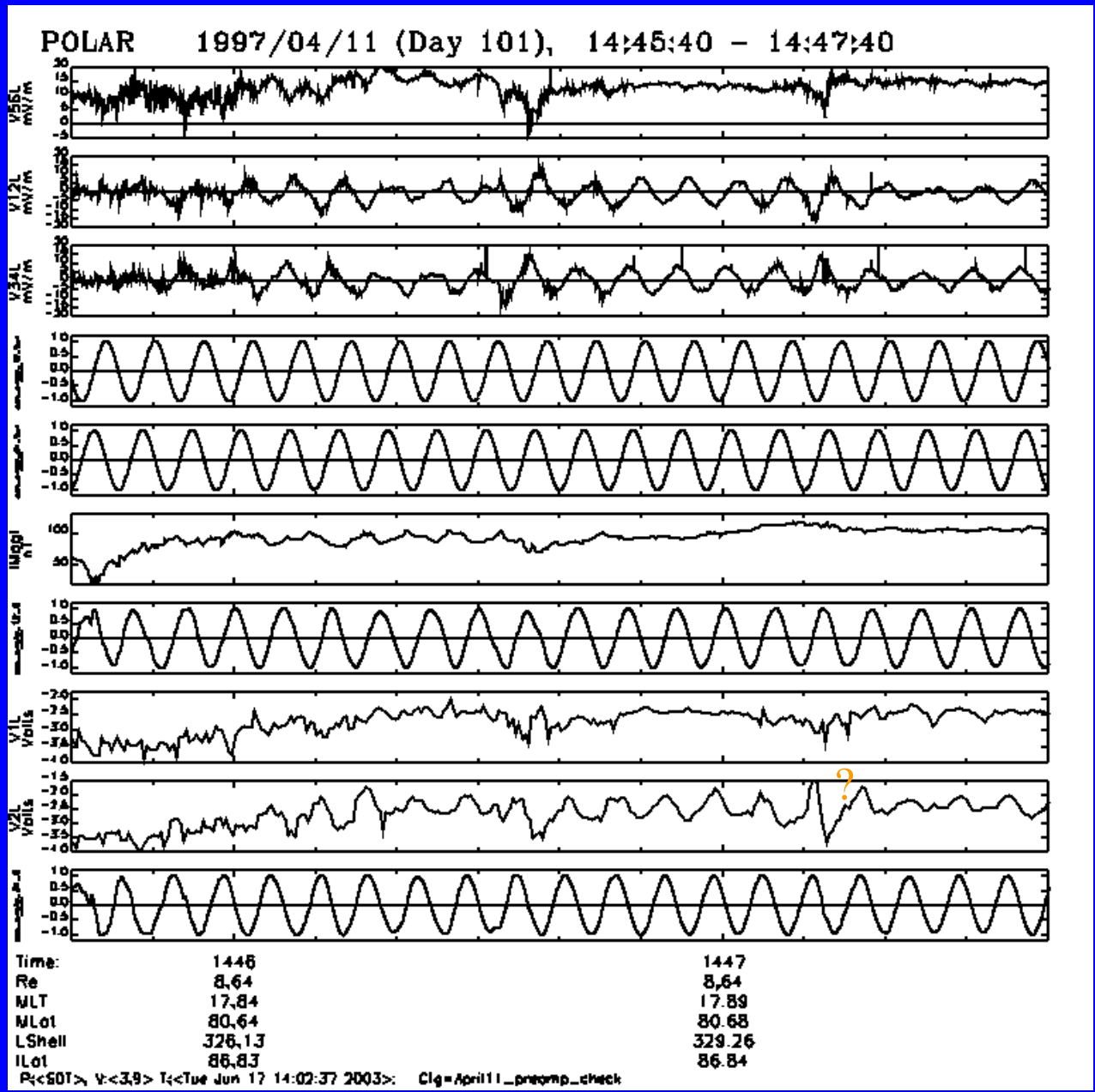
POLAR 1997/04/11 (Day 101), 14:45:40 - 14:47:40
V56L mV/m
V12L mV/m
V34L mV/m
Wagl nT
V1L Volts
V2L Volts
?
Time: 1446 1447
Re 8.64 8.64
MLT 17.84 17.89
MLat 80.64 80.68
LShell 326.13 329.26
ILat 86.83 86.84
P:<SOT>, V:<3.9> T:<Tue Jun 17 14:02:37 2003>: Cfg=April11_preamp_check

Event C

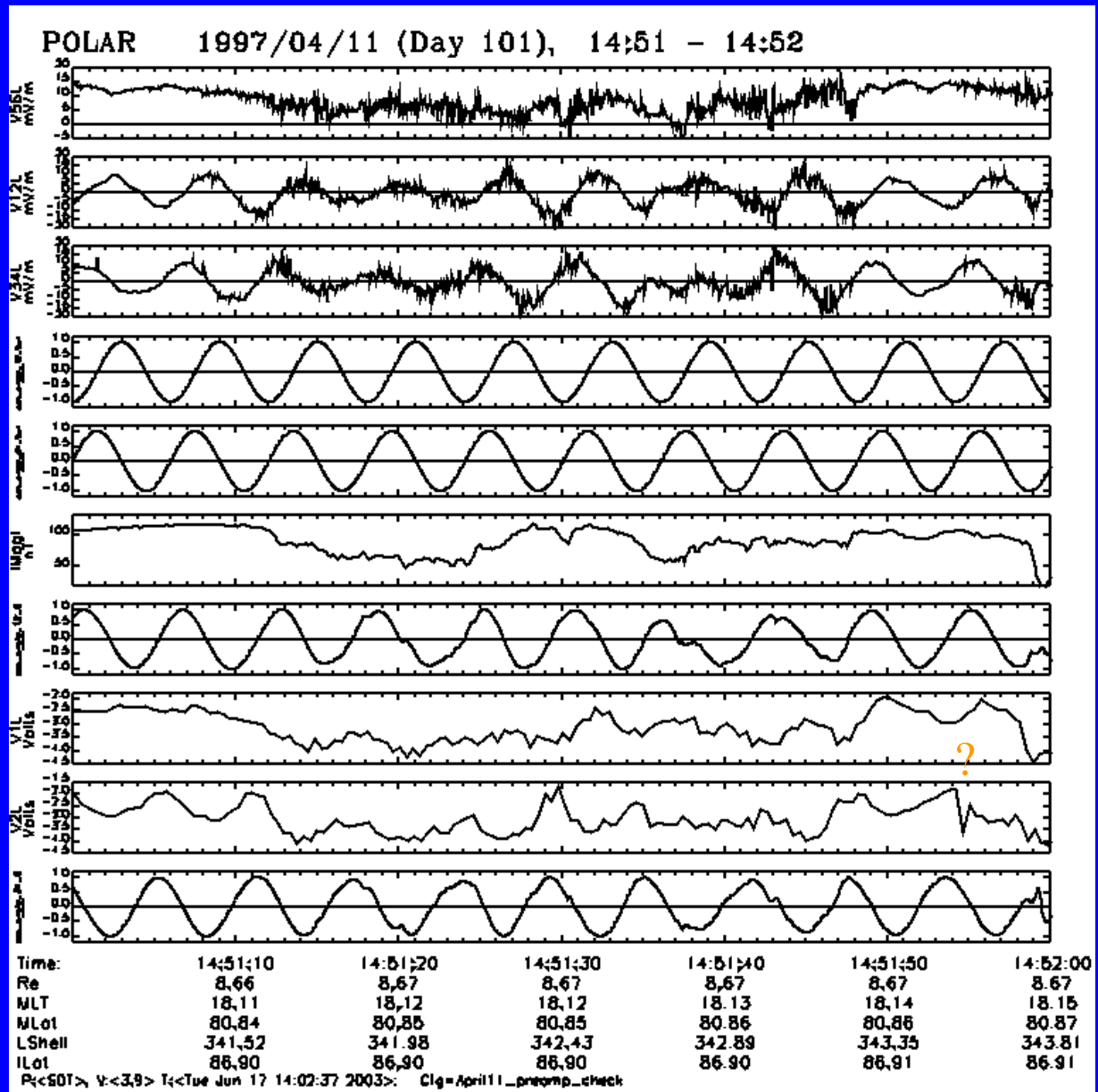
POLAR 1997/04/11 (Day 101), 14:51 - 14:52
V56L mV/m
V12L mV/m
V34L mV/m
Mggl nT
V1L Volts
V2L Volts
?
Time: 14:51:10 14:51:20 14:51:30 14:51:40 14:51:50 14:52:00
Re 8.66 8.67 8.67 8.67 8.67 8.67
MLT 18.11 18.12 18.12 18.13 18.14 18.15
MLat 80.84 80.85 80.85 80.86 80.86 80.87
LShell 341.52 341.98 342.43 342.89 343.35 343.81
ILat 86.90 86.90 86.90 86.90 86.91 86.91
P:<SDT>, V:<3.9> T:<Tue Jun 17 14:02:37 2003>: Cfg=April11_preamp_check

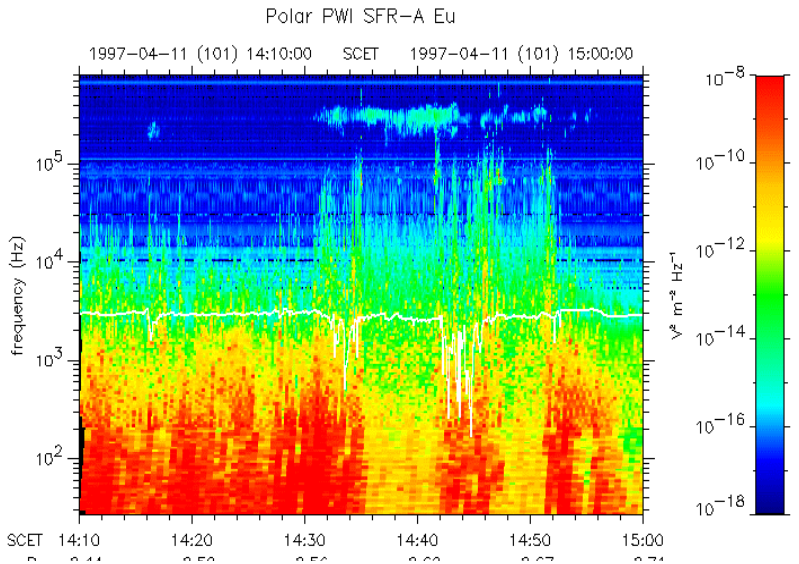

Electric component

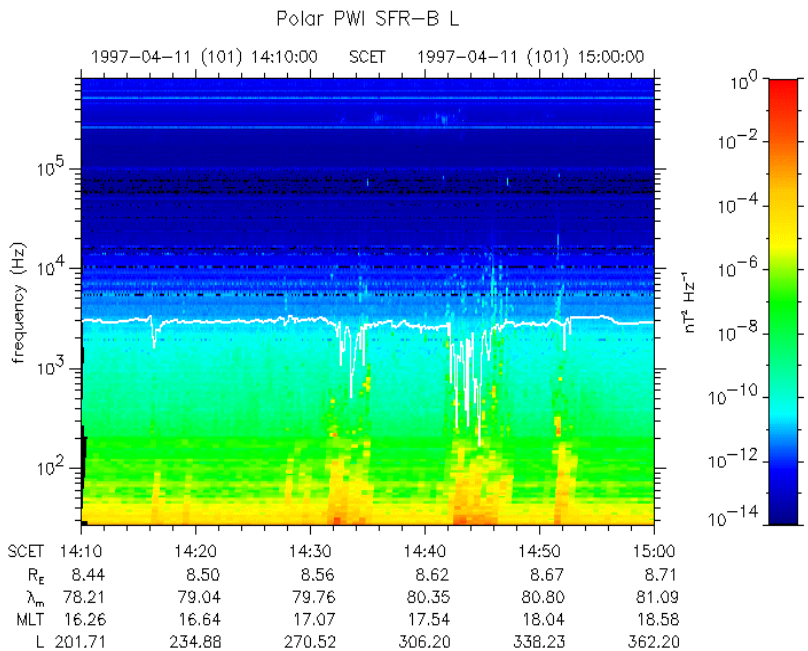

Magnetic component

MP out- Case A

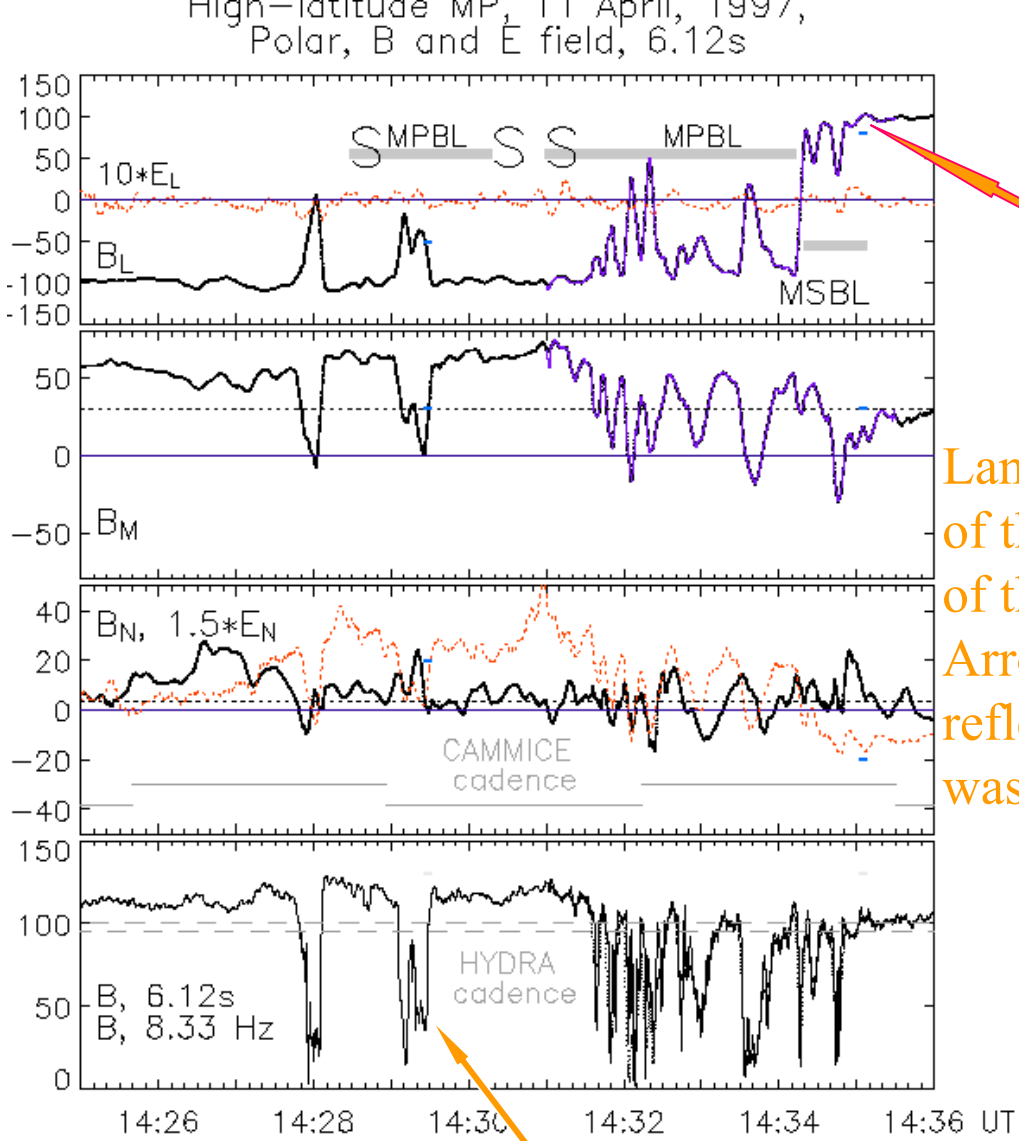

Langmuir waves are seen at the very edge of the MSBL (ion separatrix of the reconnection outflow region in MS?) Arrow shows the position where the reflected ion beam shown on previous slid was observed (*marked by blue dot*).

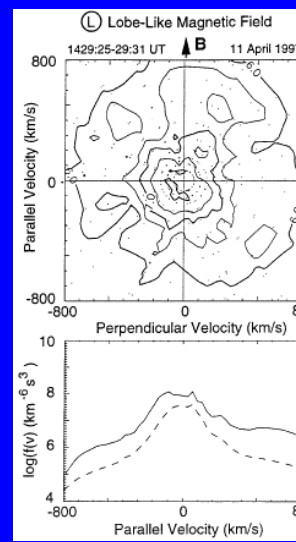

Inside and at the wall of the magnetic depression region ions are hot, stagnating, with an apparent hot high-energy beam (?). (here B increases from 40 nT to 120 nT)

(higher time resolution necessary)

Numerical simulation of magnetic field dissipation in a collisionless thin current sheet predict **suprathermal electron** production both in reconnection and reconnection-free scenarios.

We found that large-scale structures in the boundary layer are more compatible with classical reconnection picture, while micro-structures as pin-pointed by WBR wave data fit as well the reconnection free scenario, e.g., *of Shinohara et al. (2001, Phys. Rev. Lett.)*

References

-***Pickett, J. et al***., J. Geophys. Res., 106, p. 19081, 2001

-***Decreau, P. et al***., Ann. Geophys., 19, p. 1241, 2001

-***Schriver et al***., J. Geophys. Res., 105, p. 12919, 2000

-***Cattell, C. et. al***., Geophys. Res., Lett., 29, No. 5, 2002

-***Drake, J., et al***., Science, 299, p. 873, 2003

-***Shay, M., et al***., J. Geophys. Res., 106, p. 3759, 2001

-***Rogers, B., et al***., Geophys. Res., Lett., 27, No. 27, 2000

-***Drake, J., et al***., Geophys. Res., Lett., 24, No. 22, 1997

-***Drake, J., et al***., Phys. Rev. Lett., 73, No. 9, 1994

-***Berthomier et al***., "Scaling of 3D solitary waves", EGS 2003, Nice

-***Chen et al.,*** "How weak can the magnetic field be for the BGK electro holes to exist?", EGS 2003, Nice, abstract

-***Shinohara et al***., Phys. Rev. Lett., 87, No. 9, 2001

-***Russell , C.T., et al.,*** J. Geophys. Res.,105, A3, 2000

-***Le, G., et al***., J. Geophys. Res.,106, p.21083, 2001

-***Fuselier, S.A, et al.,*** J. Geophys. Res.,105, A1, 2000

-***Omura, Y., et al***., J. Geophys. Res.,101, A2, 1996